17β-HSD type 12-like is responsible for maturation-inducing hormone synthesis during oocyte maturation in masu salmon[1,2]

[1]Supported by JSPS (Japan Society for the Promotion of Science) KAKENHI Grant #21228005 (Sequencing part), #24658165 and #26252030 (Isolation and characterization of 20β-HSD).
[2]Presented in part at the 17th International Congress of Comparative Endocrinology, 15-19 July 2013, Universitat de Barcelona, Spain.

Shigeho Ijiri[3], Yasushi Shibata[4], Nonoha Takezawa[3], Yukinori Kazeto[5], Naoki Takatsuka[3], Erika Kato[3], Seishi Hagihara[3], Yuichi Ozaki[5], Shinji Adachi[3*], Kohei Yamauchi[6], and Yoshitaka Nagahama[6*].

Endocrinology (2017) 158(3): 627-639. DOI: https://doi.org/10.1210/en.2016-1349
Published: 14 December 2016

[3]Division of Marine Life Sciences, Graduate School of Fisheries Sciences, Hokkaido University, Hakodate, Hokkaido 041-8611, Japan
[4]School of Aquatic and Fishery Science, University of Washington, Seattle, Washington
[5]National Research Institute of Aquaculture, Fisheries Research Agency, Watarai, Mie, Japan
[6] South Ehime Fisheries Research Center, Ehime University, Matsuyama, Ehime, Japan

Abbreviated title: 17β-HSD12-like responsible for DHP production
Key terms: 17α,20β-dihydroxy-4-pregnen-3-one, 20β-hydroxysteroid dehydrogenase, 17β-hydroxysteroid dehydrogenase, Oocyte maturation, Granulosa, Masu salmon, *Oncorhynchus masou*

Word count: 5347
Number of figures and tables: 7 figures

Corresponding authors and people to who reprint requests should be addressed:
Yoshitaka Nagahama
Institution for Collaborative Relations
Ehime University
Bunkyo-cho 3, Matsuyama, Ehime 790-5877, Japan
Phone: 81 89 927 8513
Fax: 81 89 927 8820

e-mail: nagahama.yoshitaka.mh@ehime-u.ac.jp

Shinji Adachi
Division of Marine Life Sciences, Graduate School of Fisheries Sciences
Hokkaido University
Minato-cho 3-1-1, Hakodate, Hokkaido 041-8611, Japan
Phone: 81 138 40 5545
Fax: 81 138 40 5545
e-mail: s-adachi@fish.hokudai.ac.jp

Disclosure statement: The authors have nothing to disclose.

Abstract

The maturation-inducing hormone 17α,20β-dihydroxy-4-pregnen-3-one (DHP) was first identified in the amago salmon. However, although carbonyl reductase-like 20β-hydroxysteroid dehydrogenase (CR/20β-HSD) was reported to convert 17α-hydroxyprogesterone (17OHP) to DHP in rainbow trout, we previously found that CR/20β-HSD mRNA was not up-regulated in stimulated granulosa cells from masu salmon, which suggested that DHP is synthesized by a different enzyme. Accordingly, the present study aimed to identify the specific 20β-hydroxysteroid dehydrogenase (20β-HSD) responsible for DHP production by granulosa cells during final oocyte maturation in masu salmon. RNA-sequencing was performed on granulosa layers that were isolated from ovarian follicles at one month before ovulation and incubated with or without forskolin, which was used to mimic luteinizing hormone, and ~12 million reads were obtained, which yielded 71,062 contigs of > 100 bp. tBlastx analysis identified one contig (*#f103496*) as similar to 17β-hydroxysteroid dehydrogenase type 12 (hsd17β12); however, because the full-length *#f103496* sequence was different from hsd17β12, it was termed to hsd17β12-like (hsd17β12l). We found that mammalian cells transfected with full-length *hsd17β12l* exhibited considerable 20β-HSD activity, as indicated by efficient conversion of exogenous 17OHP to DHP. In addition, we found that *hsd17β12l* mRNA levels were consistently low in follicles during vitellogenic growth; however, the levels increased significantly during final oocyte maturation. The levels of *hsd17β12l* mRNA were also considerably increased in granulosa layers in which 20β-HSD activity was induced by salmon pituitary extract. Therefore, we suggest that hsd17β12l, not CR/20β-HSD, is the 20β-HSD responsible for DHP production by granulosa cells in masu salmon during final oocyte maturation.

Introduction

For the first time in any vertebrate, the maturation-inducing hormone was identified as 17α,20β-dihydroxy-4-pregnen-3-one (DHP) in the amago salmon in 1985 (1). Since then, many efforts have been made to identify the 20β-hydroxysteroid dehydrogenase enzyme (20β-HSD) responsible for synthesizing DHP from 17α-hydroxyprogesterone (17OHP). Unexpectedly, strong 20β-HSD activity for the substrate 17OHP was detected in the cytosol fractions of neonatal, but not mature, pig testis (2) and purified to homogeneity (3). Subsequently, partial amino acid sequences of the purified enzyme were determined, and a cDNA encoding the protein has been isolated and characterized (4). Using the pig 20β-HSD cDNA as a probe, an ortholog was also isolated from the ovarian cDNA library of rainbow trout (5), and homologs have been isolated in other teleost fish as well (6, 7).

These homologous genes have been categorized as monomeric carbonyl reductase genes, which encode enzymes that possess wide substrate specificity for carbonyl compounds and are known as carbonyl reductase-like 20β-HSD (CR/20β-HSD) (5, 6). When produced in an *Escherichia coli* heterologous expression system, these enzymes exhibit weak 17OHP-to-DHP conversion activity and a much stronger affinity for non-17OHP carbonyl compounds, such as 9,10-phenanthrenequinone, cyclohexanone, and 4-nitrobenzaldehyde (6). However, the lack of strong 17OHP-to-DHP conversion activity seems inconsistent with the high concentration of DHP produced in salmonid fish during final oocyte maturation (FOM), and it also seems unlikely that CR/20β-HSD would exhibit such a wide substrate specificity if it was a truly steroidogenic enzyme responsible for oocyte maturation, which should be strictly controlled to ensure spawning success.

In salmonid fish, including the masu salmon (*Oncorhynchus masou*), a sharp increase in serum DHP occurs around FOM and during the subsequent ovulation period (8–10), and in the 1980s, a series of *in vitro* studies using salmonid ovarian follicles demonstrated the hormonal control of DHP production (8, 11–15). Those studies reported that ovarian follicles (comprised of oocytes, granulosa layers, and theca layers) acquired the ability to produce DHP after completion of vitellogenic growth in response to the release of gonadotropin (8) or exposure to dibutyryl cAMP (13). The *in vitro* studies also demonstrated that isolated theca layers produced a substantial amount of 17OHP in response to partially purified chinook salmon gonadotropin (SG-G100; see 16) exposure, but granulosa layers did not (12). Furthermore, the studies found that both theca and granulosa layers are incapable of producing DHP by themselves; however, a co-culture of both layers can be induced to produce DHP by SG-G100, and a substantial amount of DHP can be synthesized from 17OHP by isolated granulosa layers incubated with SG-G100 (12). These findings clearly indicate that DHP is synthesized in the granulosa layer from 17OHP that is produced and delivered from the theca layer. Furthermore, these studies demonstrated that the 20β-HSD activity-inducing role of gonadotropin could be replaced with dibutyryl cAMP and forskolin (an adenylate cyclase activator), indicating the involvement of an adenylate cyclase-cAMP-dependent step (12, 17, 18). The acquisition of 20β-HSD activity by granulosa layers in response to SG-G100 exposure could also be inhibited by either actinomycin D, which inhibits RNA synthesis, or cycloheximide, which inhibits protein synthesis, clearly indicating that the step requires *de novo* synthesis of the enzyme from transcriptional events (19).

However, evidence that CR/20β-HSD is responsible for the conversion of 17OHP to DHP during FOM is

yet to be reported, and it remains unclear whether changes in *CR/20β-HSD* mRNA levels coincide with changes in 20β-HSD activity in naturally developing ovarian follicles before and during FOM or whether *CR/20β-HSD* mRNA levels increase in cultures of gonadotropin- or forskolin-induced granulosa cells before FOM. Moreover, studies using cell-free systems in amago salmon (our unpublished data) and Japanese eel (20) have demonstrated that the 20β-HSD activity in ovarian follicles is mainly located in the membrane-bound fractions of mitochondria and microsomes, with lower levels detected in the cytosolic fraction, which is inconsistent with the observation of CR/20β-HSD in the cytosol of pigs (2). Therefore, it seems premature to conclude that CR/20β-HSD is responsible for DHP production in the ovarian follicles of salmonids during FOM. Accordingly, in the present study, we investigated whether the expression of *CR/20β-HSD* mRNA was associated with 20β-HSD activity in forskolin-induced granulosa cells and aimed to identify any other 20β-HSD-encoding genes that could be responsible for producing DHP in the granulosa cells of masu salmon around FOM.

Materials and Methods

Animals and sample preparations

Masu salmon (*O. masou*) were taken from the breeding stock of the Nanae Fresh-Water Laboratory, Field Science Center for Northern Biosphere, Hokkaido University, Japan. Sampling, which consisted of taking caudal vein blood samples and removing ovaries, was conducted from April to September, since FOM and ovulation normally occur between the middle and end of September. Three to five females were selected for sampling each month, between May and August, and 17 were selected during September and classified by the developmental stages of their oocytes. To isolate serum, the collected blood samples were stored at 4 C overnight, after which the serum was separated by centrifugation at 2000 ×*g* for 5 min. Ovarian follicles were isolated from the ovaries by careful dissection in ice cold trout balanced salt solution (21), and after removing yolks, the follicles were frozen in liquid nitrogen and stored at -80 C until used for RNA extraction as *in vivo* samples. All experimental procedures complied with the National and Institutional Guidelines for Care and Use of Laboratory Animals and were approved by the Animal Research Committee of Hokkaido University.

For quantitative PCR analysis, groups of 20 isolated granulosa preparations or post-ovulation follicle layers were incubated in 4 mL Ringer medium, with or without forskolin and/or salmon pituitary extract (SPE, from the pituitaries of post-ovulation chum salmon), for 18 h in 6-well non-coated plastic culture plates. Granulosa layers and post-ovulation follicle layers were immersed in RNAlater Solution (Applied Biosystems, Foster City, CA, USA) and stored at -80 C until used for RNA extraction as *in vitro* samples. Each experiment used oocytes from a single female, in order to discount the possibility of individual variation in follicle responsiveness.

For next-generation sequence analysis, granulosa layers that were sampled from different females at one month before the spawning period were subject to five different experimental treatments. Some were independently incubated in either Ringer medium, Ringer medium with 17OHP, or Ringer medium with both forskolin and 17OHP, with three replicates each, and ~50 additional granulosa layer samples were incubated independently with or without forskolin for future RNA extraction.

Measuring 20β-HSD activity

To measure 20β-HSD activity, granulosa layer preparations were collected from females with undetectable germinal vesicles, during the two months before ovulation (at two months and one month before ovulation), and after ovulation, follicle layers that consisted of both granulosa and theca layers were drawn out at 1–2 d post-ovulation. Granulosa layers were separated from the follicle layers of oocytes using forceps under a dissecting microscope, which is a technique that yields granulosa layers that are not contaminated by thecal cells, as reported by Kagawa et al. (21). Afterward, groups of five granulosa preparations and post-ovulation follicle layers were independently incubated in 1 mL Ringer medium, Ringer medium with 100 ng/mL 17OHP and either 10 μM forskolin or 100 μg/mL SPE, or Ringer medium without 17OHP and with either 10 μM forskolin or 100 μg/mL SPE, in a 24-well non-coated plastic culture plate. Three replicate incubations were conducted for each treatment, and the assays were maintained in a humidified incubator at 13 C for 36 h, after which the DHP in the media was quantified.

DHP quantification

The DHP in blood sera and media from the 20β-HSD activity assays were extracted, according to the method of Kagawa et al. (22), and DHP concentrations were measured using time-resolved fluoroimmunoassay, according to the method of Yamada et al. (23). DHP was purchased from Sigma Chemicals (St. Louis, MO, USA), and the FKA332 antibody for DHP was purchased from Cosmo-Bio Co., Ltd. (Tokyo, Japan).

Next-generation sequencing and analysis

After incubation with or without forskolin, total RNA was extracted from the granulosa layers of female #1, which exhibited the highest induction of 20β-HSD activity by forskolin, using a column-based RNA extraction kit (RNeasy Mini Kit; Qiagen, Hilden, Germany). Complementary DNA (cDNA) libraries were prepared using an mRNA-Seq-8 Sample Prep Kit (Illumina, San Diego, CA, USA), according to the manufacturer's protocol. Briefly, poly-A RNA was fragmented and reverse transcribed using random primers. Then, the cDNA fragments were ligated to Illumina adaptors, size selected, and amplified *via* PCR. Next-generation sequencing (RNA-seq) of the RNA from the control (Ringer alone) and forskolin-treated groups was conducted using a Genetic Analyzer IIx (Illumina) by Hokkaido System Science Co., Ltd. (Sapporo, Japan), according to Illumina's instructions.

After passing the cDNA sequence reads through the Illumina chastity filter to remove aberrant reads, the reads of both groups were independently assembled using Velvet version 0.7.55 (24). The resulting contigs from both groups were further assembled using CAP3 (25), as described by Iorizzo et al. (26), in order to remove redundancy and to generate consensus contigs, and the number of reads that mapped to each contig was calculated using Bowtie (27). To evaluate whether the number of reads actually reflected a difference between the mRNA levels of the control and forskolin-treated group, we examined 13 genes that had been previously identified as up-regulated under forskolin treatment (unpublished data). In addition, contigs that were only recovered from the

forskolin-treated group were analyzed using tBlastx, and one contig that encoded a 17β-hydroxysteroid dehydrogenase type 12-like sequence (*omhsd17β12l*) was selected for further analysis.

The differential expression of *omhsd17β12l* was confirmed using qPCR, and the full-length *omhsd17β12l* cDNA sequence was determined using amplification with the SMART RACE cDNA amplification Kit (Clontech, Otsu, Japan), gene-specific primers, and Phusion High-Fidelity DNA Polymerase (New England Biolabs, Ipswich, MA, USA) and sequencing with a Genetic Analyzer 3100xl (Applied Biosystems). The open reading frames and predicted molecular weights of the predicted amino acid sequences were calculated using GENETYX-WIN Version 5.1.1 (GENETYX Co., Tokyo, Japan), without considering post-translational modification.

Phylogenetic analysis

A phylogenetic tree was constructed using the neighbor-joining method with the Molecular Evolutionary Genetics Analysis (MEGA4) software (http://www.megasoftware.net), and the GenBank accession numbers for the aligned amino acid sequences were as follows: *Salmo salar* hsd17b12, BT045689; *S. salar* hsd17b3a, BT046393; *S. salar* hsd17b3b, BT046871.

Heterologous omhsd17β12l expression and activity analysis

The two forms of the *omhsd17β12l* coding region (*typeI* and *typeII*) were subcloned into pSI, an *in vitro* eukaryotic expression vector that includes an SV40 promoter (Promega Co., Madison, WI, USA), and transfections were conducted using the jetPRIME transfection reagent (Polyplus-Transfection SA, Illkirch-Graffenstaden, France), according to the manufacturer's instructions. Briefly, HEK293T cells were transfected in 12-well cell culture plates containing Dulbecco's Modified Eagles medium (Nissui Pharmaceutical, Tokyo, Japan) with 10% fetal bovine serum, 0.65 μg *omhsd17β12l*-containing pSI, 0.13 μg pAdvantage Vector (Promega), and 1.5 μL of jetPRIME reagent at 37 C. Empty pSI was used as a control, and three independent replicates were conducted for each treatment (*omhsd17β12l typeI*-pSI, *omhsd17β12l typeII*-pSI, and empty-pSI).

After transfection, the cells were pre-cultured in Dulbecco's Modified Eagles medium without fetal bovine serum for 12 h and then separately incubated with ^{3}H-labeled 17OHP (PerkinElmer, Waltham, MT, USA; 30 ng/mL; n = 9) or cold 17OHP (100 ng/mL; n = 9), as substrates for omhsd17β12l activity, for an additional 12 h. After incubation, DHP and other steroid metabolites were extracted from the media, using three extractions with dichloromethane, and the DHP concentrations of the extracted steroid metabolites from the tritiated and cold 17OHP-treated incubations were then measured, using thin-layer chromatography (TLC) and time-resolved fluoroimmunoassay, respectively. For TLC analysis, the extracted steroid metabolites were loaded onto TLC plates, separated using benzene-acetone (4:1, v/v), detected autoradiographically with X-ray film, and quantified using ImageJ (http://rsb.info.nih.gov/ij/).

Tissue-specific *omhsd17β12l* expression

Total RNA was isolated from brain, pituitary, head kidney, hind kidney, liver, spleen, heart, follicle layers

from ovaries in late vitellogenesis or FOM, and sperm-containing testis, using ISOGEN II (Nippon Gene, Tokyo, Japan). Total RNA (1 μg) from each tissue was reverse transcribed (RT) using random hexamer primers (Life Technologies Co., Carlsbad, CA, USA) and the ReverTra Ace RT enzyme (Toyobo Co., Ltd., Osaka, Japan) in 20 μL reactions, according to the manufacturer's instructions. The diluted RT reactions (10%, v/v; 2 μL) were then used as the template for PCR amplification (20 μL reactions) of both *omhsd17β12l* and *elongation factor 1α* (*ef1α*) as a control. The primers were designed to amplify fragments that included an intron/exon boundary (Supplemental Fig. 1), in order to distinguish the amplification of genomic contaminants: *omhsd17β12l* 1-forward, 5′-GAGTGAAATTTGCCCAGACATGG-3′; *omhsd17β12l* 2-reverse, 5′-CGTCCATGTTGGCTCTCAATC-3′; *ef1α* 1-forward, 5′-AAATCTGGAGACGCCGCCA-3′; *ef1α* 3-reverse, 5′-ATGGCGGACTTGGTCACCTT-3′. Ten microliters of the PCR reactions was electrophoresed on 2% agarose gels, stained with ethidium bromide, and digitally photographed under UV light.

Quantitative PCR

Total RNA was extracted from incubated granulosa layers, yolkless follicles, or post-ovulation follicle layers (i.e., *in vitro* samples), using ISOGEN II (Nippon Gene), treated with DNase, and further cleaned, using a column-based RNA extraction kit (NucleoSpin RNA II; Macherey-Nagel GmbH & Co. KG, Düren, Germany). Subsequently, 45 or 50 ng of total RNA was amplified, using a one-step qRT-PCR system (One Step SYBR Prime Script PLUS RT-PCR Kit; TaKaRa Bio, Inc., Otsu, Japan) in a final volume of 10 μL. Total RNA (1 μg) from *in vivo* yolkless follicles was reverse transcribed as described above, and diluted RT reactions (10%, v/v; 2 μL) were used as templates for 20 μL quantitative PCR (qPCR) reactions, using FastStart Universal SYBR Green Master (Roche, Basel, Switzerland) and the StepOnePlus Real-Time PCR system (Life Technologies Co.). The qPCR primer sets included one (*ef1α*) or both (*omhsd17β12l*) primers that flanked intron–exon boundaries, in order to prevent genomic amplification: *omhsd17β12l* 3-forward, 5′-ATGGACAATGGGCAGTTGTCA-3′; *omhsd17β12l* 4-reverse, 5′-TCTGGCCAACTCATTTGCGTA-3′; *ef1α* 1-forward, 5′-AAATCTGGAGACGCCGCCA-3′; *ef1α* 2-reverse, 5′-ACGGCAAAACGACCAAGGG-3′; *CR/20β-HSD typeA* forward, 5′-CCGGTGCCAATAAAGGCAT-3′; *CR/20β-HSD typeA* reverse, 5′-AGCTCCCTCACAATCGCAAG-3′; *CR/20β-HSD typeB* forward: 5′-TCATTAACAACGCTGGAATGTCC-3′, *CR/20β-HSD typeB* reverse, 5′-CCAAAAGTCTCAGTCGCATCATTTT-3′. The same primers were used for the *omhsd17β12l* typeI and typeII sequences because qPCR was incapable of distinguishing the one nucleotide difference, and separate primer sets were used for *CR/20β-HSD typeA* and *typeB* (Supplemental Fig. 1).

Statistical analysis

Paired *t*-tests were used to detect significant differences, when comparing the data of two groups, and multiple comparisons were performed using Tukey-Kramer tests or ANOVA with Fisher's *PLSD* post hoc test. The data from mRNA quantification were converted to log 10 values before analyses, and statistical analyses were performed using StatView for Windows version 5.0.1 (SAS Institute Inc., Cary, NC, USA).

Results

In vitro 20β-HSD activity and CR/20β-HSD mRNA expression

The 20β-HSD activity of granulosa layers was significantly higher when incubated with forskolin than without forskolin (n = 5, Tukey-Kramer, $P < .01$; Figure 1), as indicated by increased conversion of exogenous 17OHP to DHP, and the granulosa layers of two females (#1 and #5) exhibited especially strong 20β-HSD activity (mean ± SE; 18.0 ± 1.1 ng/mL and 17.6 ± 2.7 ng/mL, respectively; Supplemental Fig. 2). Relatively low concentrations of DHP (6–8 ng/mL) were produced in the other three females (Supplemental Fig. 2). However, non-normalized mRNA levels [Figure 1(B) and (C)] and ef1α-normalized mRNA levels (data not shown) of both CR/20β-HSD typeA and typeB were not higher in granulosa layers incubated with forskolin than in those without forskolin (n = 5; paired *t*-tests).

RNA-seq analysis

A total of 12.538 and 12.273 million reads from RNA-seq of the control and forskolin-treated granulosa layers of female #1 were approved by the chastity filter, respectively, which accounted for 639,452 and 625,907 kb of data (BioSample accession no. SAMD00056133 and SAMD00056134, respectively). The average read length was 51 bp, and Velvet produced 95,091 and 80,282 contigs from the control and forskolin-treated reads, respectively. Furthermore, Velvet+CAP3 assembly yielded 40,013 mixed contigs and 35,762 and 22,150 singlets from the control and forskolin-treated Velvet contigs, respectively (mixed and singlet contig sequences are deposited in the NCBI Transcriptome Shotgun Assembly (TSA) Database, accession nos. IABA01000001– IABA01097925). Of these, ~71,000 contigs (73%) had lengths >100 bp, and the contigs had an N50 length of 181 bp, average length of 182 bp, and maximum length of 5190 bp. The number of mapped and singlet reads that were obtained from the control and forskolin-treated granulosa samples have been deposited in the NCBI Gene Expression Omnibus (GEO) Database (accession no. GSE85134).

Among the contigs, we identified 11 of the 13 genes that we had previously identified as up-regulated under forskolin treatment (unpublished data, cDNA sequence data is included in Supplemental Fig. 3), and all of those 11 genes were represented by a greater number of reads in the forskolin group (Supplemental Fig. 4), in agreement with the qPCR findings.

In addition, we also identified 953 unique contigs of >100 bp that were constructed exclusively from the forskolin-treated group reads (Supplemental data 1), and tBlastx analysis identified a 117-bp contig (*#f103496*) as a member of the 17β-hydroxysteroid dehydrogenase type 3 (hsd17β3) family (Figure 2A). One-step qPCR analysis confirmed that the expression of *#f103496* was considerably higher in the forskolin-treated granulosa layers than in the control group (n = 5, females #1–5, paired *t*-tests; $P < .0005$; Figure 2C), whereas the levels of *ef1α* mRNA were not different between the two groups, and the *ef1α*-normalized level of *#f103496* expression was also greater in the forskolin group than in the control group (n = 5, paired *t*-tests; $P < .0005$; Figure 2D).

Full-length *#f103496* cDNA analysis

The full-length *#f103496* cDNA (1622 bp) contained an open reading frame of 984 bp, which was predicted to encode a 36.7 kDa protein of 328 residues. The sequence also contained a 40-bp 5′ untranslated region, a 597-bp 3′ untranslated region, and a terminal polyadenylation sequence. Furthermore, we identified two forms of cDNA open reading frame sequences (*typeI* and *typeII*), which differed by a single nucleotide (A or G at position 718; Figure 3A) that altered the Lys residue at position 226 to Arg (AC149904 and LC149905, respectively). Phylogenetic analysis, using amino acid sequences, placed the full-length *#f103496* between the *S. salar* hsd17β3 and hsd17β12 clusters (Figure 3B), and the nucleotide sequence identities between the full-length *#f103496* open reading frame and *S. salar hsd17β12*, *hsd17β3a*, and *hsd17β3b* were 60%, 61%, and 60%, respectively.

In addition, Blastn analysis identified another contig (*#f168003*) that matched the full-length *#f103496* sequence. The number of *#f168003* reads in the control and forskolin-treated groups were 0 and 5, respectively, and the combined total of both *#f168003* and *#f103496* reads was 0 and 17, respectively (Figure 3A). Meanwhile, three other contigs (mixed_23722 (#m23722), #m27275, and #f39886) were also found to encode partial *O. masou hsd17β12* sequences. Their sequence identities against *S. salar hsd17β12* were 94%, 97%, and 97%, respectively, and the total number of #m23722, #m27275, and #f39886 reads in the control and forskolin-treated groups were 569 and 655, respectively (Figure 3C). However, no *hsd17β3*-encoding cDNA was found in the contigs from incubated *O. masou* granulosa layers. Thus, based on data described above, the full-length *#f103496* cDNA was designated as *omhsd17β12l.*

Heterologous omhsd17β12l expression and activity analysis

Thin-layer chromatography revealed that HEK293T cells transfected with *omhsd17β12l typeI* or *typeII* exhibited a strong ability to convert 17OHP to DHP (Figure 4A). In fact, the HEK293T cells transfected with *omhsd17β12l typeI* or *typeII* converted 94–97% of the ^{3}H-17OHP added to their cultures to DHP, which was significantly higher than the 7–8% conversion observed in HEK293T cells transfected with an empty vector (mock; ANOVA with Fisher's PLSD, $F_{2,6}$ = 3857.1 P < .0001; Figure 4B), and the *omhsd17β12l*-transfected cells also demonstrated higher conversion activity when exposed to 100 ng/mL (303 nmol/L) of cold 17OHP ($F_{2,6}$ = *19.4*, P < .05; Figure 4C). However, the 20β-HSD activity of *omhsd17β12l typeI* or *typeII* was not significantly different.

Tissue-specific omhsd17β12l expression

RT-PCR analysis revealed that *omhsd17β12l* mRNA was barely present in head kidney, whereas it was strongly amplified from testis and ovarian follicles at FOM. However, no amplification was detected from the RNA of brain, pituitary, hind kidney, liver, spleen, heart, or vitellogenic ovarian follicles (Figure 5A).

Seasonal variation in serum DHP and omhsd17β12l expression

The serum concentration of DHP was consistently low during vitellogenic growth, from May to early September, as were the *ef1α*-normalized *omhsd17β12l* mRNA levels of follicle layers, and this trend was also

observed for two of three females with oocytes at the migratory nucleus stage. However, the DHP serum concentration was considerably elevated in the third female with oocytes at the migratory nucleus stage (300 ng/mL), as was *ef1α*-normalized *omhsd17β12l* mRNA level in the follicle layers of the same female.

In contrast, serum DHP was highly elevated (90–250 ng/mL) in all four females with oocytes that had completed germinal vesicle breakdown (GVBD), although the *omhsd17β12l* mRNA levels were higher in the follicle layers of three of the four females than in those of the fourth female. In addition, the female whose follicle layers exhibited lower *omhsd17β12l* mRNA also exhibited a higher serum DHP concentration.

After ovulation, all five females retained DHP serum concentrations that were high, but lower than those during GVBD. However, the *omhsd17β12l* mRNA levels in the follicle layers from ovulated ovaries were low in all females (Figure 5B).

According to Tukey–Kramer analyses, the DHP concentration among the late vitellogenic, GVBD, and post-ovulation groups were significantly different from one another ($P < .05$). The *omhsd17β12l* mRNA levels of the GVBD group were also significantly different from the late vitellogenic and post-ovulation groups ($P < .05$), although there was no significant difference between the late vitellogenic and post-ovulation groups ($P > .05$).

In vitro 20β-HSD activity and omhsd17β12l expression in pre-ovulation granulosa layers

Granulosa layers from females at two months before ovulation converted significantly more 17OHP to DHP when incubated with forskolin or SPE than when incubated without (n = 4, Tukey–Kramer, $P < .01$; Figure 6A), indicating higher levels of 20β-HSD. In addition, the *omhsd17β12l* mRNA levels were significantly higher in granulosa layers incubated with forskolin and SPE, than in those incubated without (n = 4, Tukey–Kramer, $P < .01$; Figure 6B), and the *ef1α*-normalized *omhsd17β12l* mRNA levels were also higher in the forskolin and SPE groups than in the control group (n = 4, Tukey–Kramer, $P < .01$; Figure 6C). The five females sampled at one month before ovulation (#1–5; Figure 1 and 2) also yielded similar results, although we only tested the effects of forskolin (i.e., not SPE).

In the one female sampled at the migratory nucleus stage, a small amount of DHP was detected in the control and 17OHP groups (9 ng/mL and 7 ng/mL, respectively), but when forskolin or SPE were combined with 17OHP, the granulosa layers exhibited much higher levels of 20β-HSD, as indicated by substantially higher DHP concentrations (20 ng/mL and 49 ng/mL, respectively; Figure 6D). Furthermore, the raw *omhsd17β12l* mRNA level was strikingly elevated when the granulosa layers were incubated with SPE (2600 times higher than without; Figure 6E), and the *ef1α*-normalized *omhsd17β12l* mRNA level was ~1900 times higher (Figure 6F).

In vitro 20β-HSD activity and omhsd17β12l expression in post-ovulation follicle layers

The post-ovulation follicle layers from five experiments using different females produced significantly higher DHP in the presence of SPE than without (Tukey–Kramer, $P < .01$), and in the presence of 17OHP, forskolin and SPE induced higher DHP production (Tukey–Kramer, $P < .05$ and .01, respectively); however, the level of DHP production was not further enhanced by the presence of 17OHP (fors vs. 17OHP + fors, SPE vs. 17OHP + SPE;

Figure 7A). The raw *omhsd17β12l* mRNA levels were not higher in the follicle layers incubated with SPE than in those incubated in Ringer medium alone (Tukey–Kramer, $P < .05$; Figure 7B), and no significant difference was observed between the *ef1α*-normalized *omhsd17β12l* levels of follicle layers incubated in Ringer medium alone or in Ringer medium with SPE (Tukey–Kramer, $P < .05$; Figure 7C).

However, the *ef1α*-normalized *omhsd17β12l* level of the follicle layer control group (0.469 ± 0.094, n = 5) was significantly higher than that of the granulosa layer control group of vitellogenic females (0.008 ± 0.003, n = 9, Tukey-Kramer; $P < .01$) and lower than that of the SPE-treated granulosa layers of females at two months pre-ovulation (7.116 ± 3.655, n = 4, Tukey-Kramer; $P < .05$).

Discussion

Since the isolation of a cDNA encoding CR/20β-HSD from pig (4), many studies have targeted CR/20β-HSD orthologs as being responsible for maturation-inducing hormone (MIH) synthesis (7, 28–32). Some studies demonstrated weak 20β-HSD activity of CR/20β-HSD towards 17OHP (7, 30), whilst others did not check its activity (28, 29, 31, 32). Moreover, several reports used the gene name 20β-HSD without even using the prefix CR (29–31). In this study, we do not find support for crediting CR/20β-HSD with MIH production but instead present compelling evidence that 17β-HSD type 12-like is the enzyme responsible for DHP production in masu salmon. Accordingly, we urge researchers who study the regulation of MIH production during FOM in other teleosts to reconsider whether CR/20β-HSD is suitable for that purpose.

Relationship between 20β-HSD activity and CR/20β-HSD mRNA levels in cultured granulosa cells

Previous studies identified two forms of *CR/20β-HSD* from rainbow trout and demonstrated that one form (*typeA*) exhibited weak 20β-HSD activity when offered 17OHP, whereas the other (*typeB*) did not have any 20β-HSD activity. (5). In the present study, we found that the mRNA levels of both *CR/20β-HSD typeA* and *typeB* in forskolin-induced granulosa were no greater than the levels observed in the control group. This result was inconsistent with a previous study that reported that the induction of 20β-HSD activity in granulosa cells requires *de novo* mRNA synthesis (19). The only other relevant *in vivo* study reported 7-fold increases in the *CR/20β-HSD* mRNA levels of follicles during sexual maturation of rainbow trout (33). However, the *CR/20β-HSD* autoradiograph band of the study's northern blot analysis (per 100 ng of poly(A) RNA) failed to indicate a substantial increase in *CR/20β-HSD* mRNA during the final maturation period. These findings, together with those from the present study, prompt us to conclude that *CR/20β-HSD* does not encode the 20β-HSD that is responsible for DHP production during the period of oocyte maturation in salmonid species.

Characterization of 17β-HSD type 12-like

In the present study, RNA-seq analysis identified one contig (*#f103496*) as encoding a putative hydroxysteroid dehydrogenase from among 953 contigs that were constructed exclusively from the forskolin-treated group reads. The full-length *#f103496* sequence was placed between Atlantic salmon (*S. salar*) hsd17β3 and

hsd17β12 but did not seem orthologous to either. Rather, a substantial number of reads mapped to three contigs that matched *S. salar hsd17β12*, but this number was comparable in both the control and forskolin groups, suggesting that *hsd17β12* does not play a role in 20β-HSD activity. Although we were unable to locate a contig that sufficiently matched *S. salar hsd17β3a* and *3b*, full-length *#f103496* is obviously not an *hsd17β3* ortholog, since full-length *#f103496* and *S. salar hsd17β3* exhibit low sequence identity (only 35–36% amino acid identity). Therefore, we suggest that *#f103496* differs from *hsd17β12* and *hsd17β3* and have designated the gene as *omhsd17β12-like* (*omhsd17β12l*).

Mindnich et al. (34) recently identified a novel 17β-HSD-like enzyme similar to *hsd17β3* and *hsd17β12* in the zebrafish genome. The group demonstrated that the enzyme was able to convert cortisone to 20β-hydroxycortisone and accordingly named the gene *20β-HSD type2* (*hsd20β2*)(35). Subsequently, *omhsd17β12l* was classified in the *hsd20β2* subcluster in a phylogenetic tree built by Tokarz et al. (35). Therefore, *omhsd17β12l* is considered a masu salmon ortholog of zebrafish *hsd20β2* (*drhsd20β2*).

The present study clearly demonstrated that both omhsd17β12l typeI and typeII exhibited considerable 20β-HSD activity, converting 17OHP to DHP in high yields. Furthermore, the expression of *omhsd17β12l* was strictly limited to maturing ovaries and sperm-containing testis, which may indicate that omhsd17β12l is involved in reproduction-related steroid synthesis in masu salmon. In zebrafish, 20β-HSD activity of drhsd20β2 towards 17OHP has not yet been examined; nevertheless, the authors suggested that drhsd20β2 was not likely to play a role in reproduction-related steroid biosynthesis, owing to its ubiquitous expression pattern in all the tissues examined, both in adult fish and throughout embryogenesis (35).

Changes in serum DHP and omhsd17β12l mRNA levels during sexual maturation

The serum DHP concentration and *omhsd17β12l* mRNA levels in the follicle layers were largely well-correlated, but the odd exception was evident; thus, although all four post-GVBD females exhibited elevated serum DHP levels, a notable increase in *omhsd17β12l* transcript abundance in the follicle layers was observed in only three of the fish, *omhsd17β12l* mRNA levels remaining relatively low in the fourth female. This inconsistency can be attributed to the degradation of *omhsd17β12l* transcripts, which may occur rapidly after expression. In fact, such inconsistencies between serum DHP and *omhsd17β12l* expression were also observed in the follicles of post-ovulation females. Serum DHP concentrations remained relatively high in all five post-ovulation females, but the *omhsd17β12l* transcripts were relatively low, again suggesting that the expression of *omhsd17β12l* is temporal and only exists for a short time span. In contrast, omhsd17β12l protein and serum DHP can persist for relatively long periods.

Relationship between induction of 20β-HSD activity and up-regulation of omhsd17β12l mRNA expression *in vitro*

Our present *in vitro* investigation showed a close relationship between the induction of 20β-HSD activity and up-regulation of *omhsd17β12l* mRNA by forskolin and SPE in granulosa layers at one or two months before

ovulation. Human chorionic gonadotropin (HCG) exhibited similar effects as the forskolin and SPE treatments (Supplemental Figure 5), making it reasonable to assume that forskolin and SPE are mimicking luteinizing hormone stimulation. After the migratory nucleus stage, in most follicles, the connection between granulosa layers and the oocyte membrane becomes loose (reduced inter-digitation), which allows granulosa layers to be manually removed along with theca layers. Therefore, granulosa layers were only successfully separated from a single female at the migratory nucleus stage. Although statistical analysis was not possible, we found that the *omhsd17β12l* mRNA level was drastically elevated in the presence of SPE, by over 10 times that of granulosa layers from one or two months before ovulation. This indicates that the responsiveness of *omhsd17β12l* transcription to induction increases further during the FOM period. However, the 20β-HSD activity of the migratory nucleus-stage granulosa layer was not elevated as drastically as the up-regulation of *omhsd17β12l*. Therefore, changes in 20β-HSD activity and *omhsd17β12l* mRNA levels of incubated granulosa cells apparently do not exhibit a linear relationship. This suggests that post-transcriptional and/or post-translational regulation may exist over and beyond the principal regulation by transcription.

In the post-ovulation follicle layers, DHP production could still be induced by SPE stimulation, whereas *omhsd17β12l* expression could not. This observation is consistent with our previous report that 20β-HSD activity becomes non-inducible in the post-ovulation granulosa layers of amago salmon (11). The increased DHP production by ovulated follicle layers is probably caused by stimulated 17OHP production in the theca rather than by induction of 20β-HSD activity; indeed, addition of exogenous 17OHP (SPE vs. SPE + 17OHP) did not further increase DHP production beyond that achieved with SPE only, as was reported from amago salmon previously (11). Both 20β-HSD activity and *omhsd17β12l* expression thus appear to have become insensitive to induction by SPE and the gene may have been silenced after its activation during FOM. Furthermore, we also found that the levels of *omhsd17β12l* mRNA in the control incubations of post-ovulation follicles remained relatively high, when compared with the *omhsd17β12l* mRNA levels of granulosa layers from females at one and two months before ovulation, which suggests that detectable levels of *omhsd17β12l* mRNA remain in the ovulated follicles. Accordingly, post-ovulation follicles retain 20β-HSD activity.

Future directions

To date, fourteen different types of 17β-HSD have been identified in mammals (36). Some of these are known to be multifunctional because of their preference for diverse substrates, extending well beyond steroids (37, 38). Moreover, human HSD17B2 was shown to have 20α-HSD (oxidase) activity using 20α-progesterone as substrate, aside from its catalytic 17β-HSD (oxidase) activity with estradiol and testosterone (39, 40). We have now demonstrated profound 20β-HSD activity by omhsd17β12l, resulting in DHP production, yet, we have retained the term hsd17β as the gene name in view of its possible multifunctionality. However, if 20β-HSD activity of hsd17β12l orthologs are conserved among other taxa, then it should be renamed as hsd20β. Such characterization of hsd17β12l in other species is currently in progress.

Acknowledgements

We would like to thank Etsuro Yamaha at the Nanae Fresh-Water Laboratory for providing masu salmon.

References

1. Nagahama Y, Adachi S. Identification of maturation-inducing steroid in a teleost, the amago salmon (*Oncorhynchus rhodurus*). Dev Biol 1985; 109:428-435.
2. Nakajin S, Ohno S, Takahashi M, Nishimura K, Shinoda M. 20β-hydroxysteroid dehydrogenase of neonatal pig testis: Localization in cytosol fraction and comparison with the enzyme from other species. Chemi Pharm Bull 1987; 35:2490-2494.
3. Nakajin S, Ohno S, Shinoda M. 20β-hydroxysteroid dehydrogenase of neonatal pig testis: Purification and some properties. J Biochem 1988; 104:565-569.
4. Tanaka M, Ohno S, Adachi S, Nakajin S, Shinoda M, Nagahama Y. Pig testicular 20β-hydroxysteroid dehydrogenase exhibits carbonyl reductase-like structure and activity. cDNA cloning of pig testicular 20β-hydroxysteroid dehydrogenase. J Biol Chem 1992; 267:13451–13455.
5. Guan GJ, Tanaka M, Todo T, Young G, Yoshikuni M, Nagahama Y. Cloning and expression of two carbonyl reductase-like 20β-hydroxysteroid dehydrogenase cDNAs in ovarian follicles of rainbow trout (*Oncorhynchus mykiss*). Biochem Bioph Res Co 1999; 255:123–128.
6. Tanaka M, Nakajin S, Kobayashi D, Fukada S, Guan GJ, Todo T, Senthilkumaran B, Nagahama Y. Teleost ovarian carbonyl reductase-like 20β-hydroxysteroid dehydrogenase: Potential role in the production of maturation-inducing hormone during final oocyte maturation. Biol Reprod 2002; 66:1498–1504.
7. Senthilkumaran B, Sudhakumari CC, Chang XT, Kobayashi T, Oba Y, Guan G, Yoshiura Y, Yoshikuni M, Nagahama Y. Ovarian carbonyl reductase-like 20β-hydroxysteroid dehydrogenase shows distinct surge in messenger RNA expression during natural and gonadotropin-induced meiotic maturation in Nile tilapia. Biol Reprod 2002; 67:1080–1086.
8. Young G, Crim LW, Kagawa H, Kambegawa A, Nagahama Y. Plasma 17α,20β-dihydroxy-4-pregnen-3-one levels during sexual-maturation of amago salmon (*Oncorhynchus-rhodurus*): Correlation with plasma gonadotropin and in vitro production by ovarian follicles. Gen Comp Endocrinol 1983; 51:96–105.
9. Scott AP, Sumpter JP, Hardiman PA. Hormone changes during ovulation in the rainbow-trout (*Salmo gairdneri* Richardson). Gen Comp Endocrinol 1983; 49:128–134.
10. Yamauchi K, Kagawa H, Ban M, Kasahara N, Nagahama Y. Changes in plasma estradiol-17βand 17α,20β-dihydroxy-4-pregnen-3-one levels during final oocyte maturation of the masu salmon *Oncorhynchus-masou*. B Jpn Soc Sci Fish 1984; 50:2137–2137.
11. Kanamori A, Adachi S, Nagahama Y. Developmental changes in steroidogenic responses of ovarian follicles of amago salmon (*Oncorhynchus-rhodurus*) to chum salmon gonadotropin during oogenesis. Gen Comp Endocrinol 1988; 72:13–24.
12. Young G, Adachi S, Nagahama Y. Role of ovarian thecal and granulosa layers in gonadotropin-induced

synthesis of a salmonid maturation-inducing substance (17α,20β-dihydroxy-4-pregnen-3-one). Dev Biol 1986; 118:1–8.

13. Young G, Ueda H, Nagahama Y. Estradiol-17β and 17α,20β-dihydroxy-4-pregnen-3-one production by isolated ovarian follicles of amago salmon (*Oncorhynchus rhodurus*) in response to mammalian pituitary and placental hormones and salmon gonadotropin. Gen Comp Endocrinol 1983; 52:329–335.
14. Nagahama Y. Gonadotropin action on gametogenesis and steroidogenesis in teleost gonads. Zool Sci 1987; 4:209–222.
15. Nagahama Y. Cytodifferentiation of ovarian follicle cells during oocyte growth and maturation. Cell Differ Dev 1988; 25 Supplement:9–14.
16. Donaldson EM, Yamazaki F, Dye HM, Philleo WW. Preparation of gonadotropin from salmon (*Oncorhynchus tshawytscha*) pituitary glands. Gen Comp Endocrinol 1972; 18:469–481.
17. Nagahama Y, Kagawa H, Adachi S, Young G. Stimulation of 17α, 20β-dihydroxy-4-pregnen-3-one production in the granulosa cells of amago salmon, *Oncorhynchus rhodurus*, by cyclic nucleotides. J Exp Zool 1985; 236:371–375.
18. Kanamori A, Nagahama Y. Involvement of 3',5'-cyclic adenosine monophosphate in the control of follicular steroidogenesis of amago salmon (*Oncorhynchus rhodurus*). Gen Comp Endorcinol 1988; 72:39–53.
19. Nagahama Y, Young G, Adachi S. Effect of actinomycin D and cycloheximide on gonadotropin-induced 17α, 20β-dihydroxy-4-pregnen-3-one production by intact ovarian follicles and granulosa cells of the amago salmon, *Oncorhynchus rhodurus*. Dev Growth Differ 1985; 27:213–221.
20. Kazeto Y, Adachi S, Yamauchi K. 20β-hydroxysteroid dehydrogenase of the Japanese eel ovary: Its cellular localization and changes in the enzymatic activity during sexual maturation. Gen Comp Endocrinol 2001; 122:109–115.
21. Kagawa H, Young G, Adachi S, Nagahama Y. Estradiol-17β production in amago salmon (*Oncorhynchus rhodurus*) ovarian follicles: Role of the thecal and granulosa cells. Gen Comp Endocrinol 1982; 47:440–448.
22. Kagawa H, Takano K, Nagahama Y. Correlation of plasma estradiol-17β and progesterone levels with ultrastructure and histochemistry of ovarian follicles in the white-spotted char, *Salvelinus leucomaenis*. Cell Tissue Res 1981; 218:315–329.
23. Yamada H, Satoh R, Ogoh M, Takaji K, Fujimoto Y, Hakuba T, Chiba H, Kambegawa A, Iwata M. Circadian changes in serum concentrations of steroids in Japanese char *Salvelinus leucomaenis* at the stage of final maturation. Zool Sci 2002; 19:891–898.
24. Zerbino DR, Birney E. Velvet: Algorithms for de novo short read assembly using de Bruijn graphs. Genome Res 2008; 18:821–829.
25. Huang XQ, Madan A. CAP3: A DNA sequence assembly program. Genome Res 1999; 9:868–877.
26. Iorizzo M, Senalik DA, Grzebelus D, Bowman M, Cavagnaro PF, Matvienko M, Ashrafi H, Van Deynze A, Simon PW. De novo assembly and characterization of the carrot transcriptome reveals novel genes, new markers, and genetic diversity. BMC Genomics 2011; 12:389.

27. Langmead B, Trapnell C, Pop M, Salzberg SL. Ultrafast and memory-efficient alignment of short DNA sequences to the human genome. Genome Biol 2009; 10:R25.

28. Wang YJ, Ge W. Cloning of zebrafish ovarian carbonyl reductase-like 20β-hydroxysteroid dehydrogenase and characterization of its spatial and temporal expression. Gen Comp Endocrinol 2002; 127:209–216.

29. Mittelholzer C, Andersson E, Consten D, Hirai T, Nagahama Y, Norberg B. 20β-hydroxysteroid dehydrogenase and CYP19A1 are differentially expressed during maturation in Atlantic cod (*Gadus morhua*). J Mol Endocrinol 2007; 39:319–328.

30. Sreenivasulu G, Senthilkumaran B. New evidences for the involvement of 20β-hydroxysteroid dehydrogenase in final oocyte maturation of air-breathing catfish. Gen Comp Endocrinol 2009; 163:259–269.

31. Jeng SR, Yueh WS, Lee YH, Yen HF, Chang CF. 17,20β,21-Trihydroxy-4-pregnen-3-one biosynthesis and 20β-hydroxysteroid dehydrogenase expression during final oocyte maturation in the protandrous yellowfin porgy, *Acanthopagrus latus*. Gen Comp Endocrinol 2012; 176:192–200.

32. Zapater C, Chauvigne F, Scott AP, Gomez A, Katsiadaki I, Cerda J. Piscine follicle-stimulating hormone triggers progestin production in gilthead seabream primary ovarian follicles. Biol Reprod 2012; 87:1–13.

33. Nakamura I, Evans JC, Kusakabe M, Nagahama Y, Young G. Changes in steroidogenic enzyme and steroidogenic acute regulatory protein messenger RNAs in ovarian follicles during ovarian development of rainbow trout (*Oncorhynchus mykiss*). Gen Comp Endocrinol 2005; 144:224–231.

34. Mindnich, R; Deluca, D; Adamski, J. Identification and characterization of 17β-hydroxysteroid dehydrogenases in the zebrafish, *Danio rerio*. Mol Cell Endocrinol 2004; 215:19–30.

35. Tokarz J, Mindnich R, Norton W, Moeller G, de Angelis MH, Adamski J. Discovery of a novel enzyme mediating glucocorticoid catabolism in fish: 20β-Hydroxysteroid dehydrogenase type 2. Mol Cell Endocrinol 2012; 349:202–213.

36. Marchais-Oberwinkler S, Henn C, Moller G, Klein T, Negri M, Oster A, Spadaro A, Werth R, Wetzel M, Xu KY, Frotscher M, Hartmann RW, Adamski J. 17β-hydroxysteroid dehydrogenases (17β-HSDs) as therapeutic targets: Protein structures, functions, and recent progress in inhibitor development. J Steroid Biochem Mol Biol 2011; 125:66–82.

37. Moeller G, Adamski J. Multifunctionality of human 17β-hydroxysteroid dehydrogenases. Mol Cell Endocrinol 2006; 248:47–55.

38. Moeller G, Adamski J. Integrated view on 17β-hydroxysteroid dehydrogenases. Mol Cell Endocrinol 2009; 301:7–19.

39. Puranen TJ, Kurkela RM, Lakkakorpi JT, Poutanen MH, Itaranta PV, Melis JPJ, Ghosh D, Vihko RK, Vihko PT. Characterization of molecular and catalytic properties of intact and truncated human 17β-hydroxysteroid dehydrogenase type 2 enzymes: Intracellular localization of the wild-type enzyme in the endoplasmic reticulum. Endocrinology 1999; 140: 3334–3341.

40. Wu L, Einstein M, Geissler WM, Chan HK, Elliston KO, Andersson S. Expression cloning and characterization of human 17β-hydroxysteroid dehydrogenase type-2, a microsomal-enzyme possessing 20α-hydroxysteroid

dehydrogenase-activity. J Biol Chem 1993; 268: 12964–12969.

Supplemental figure legends

Supplemental Fig. 1. qPCR primer sets used for ef1α, omhsd17β12l, and CR/20β-HSD typeA and typeB.

Supplemental Fig. 2. Production of 17α,20β-dihydroxy-4-pregnen-3-one (DHP) by isolated granulosa layers from females #1–5. Vertical bars represents the means ± SD (n = 3).

Supplemental Fig. 3. Complementary DNA sequences and primer sets used for qPCR of 13 genes that were identified as up-regulated under forskolin treatment by cDNA subtraction analysis.

Supplemental Fig. 4. The number of mapped reads and cDNA levels in incubated granulosa layers and the mRNA levels of previously identified forskolin-induced genes in *in vivo* sampled follicle layers. The number of reads represents the total number of reads mapped to cDNA sequences from the control and forskolin-treated groups (A, B). Relative cDNA levels were measured by quantitative PCR, using 50 ng of amplified cDNA that was prepared from incubated granulosa layers (C), and the expression level of each gene was normalized using *ef1α* mRNA levels in 45 ng of total RNA from follicle layers collected from *in vivo* samples collected from a single female at each developmental stage (D).

Supplemental Fig. 5. 20β-Hydroxysteroid dehydrogenase activity and *omhsd17β12l* mRNA levels in incubated granulosa layers of a single female, at one month before ovulation. Incubations were conducted in Ringer medium with no additives (cont) or 100 ng/mL 17α-hydroxyprogesterone (17OHP), or a combination of 17OHP and human chorionic gonadotropin (HCG; 100 IU/mL; Nippon Zenyaku Kogyo Co., Ltd., Koriyama, Fukushima, Japan). The post-incubation concentrations of 17α,20β-dihydroxy-4-pregnen-3-one (DHP) in the incubation media are represented as the mean ± SD of three replicate incubations (A). Levels of o*mhsd17β12l* and *ef1α* mRNA in 45 ng of total RNA from granulosa layers incubated in Ringer medium (cont, open columns) or with HCG (gray column) (B). *ef1α*-Normalized *omhsd17β12l* mRNA levels (C).

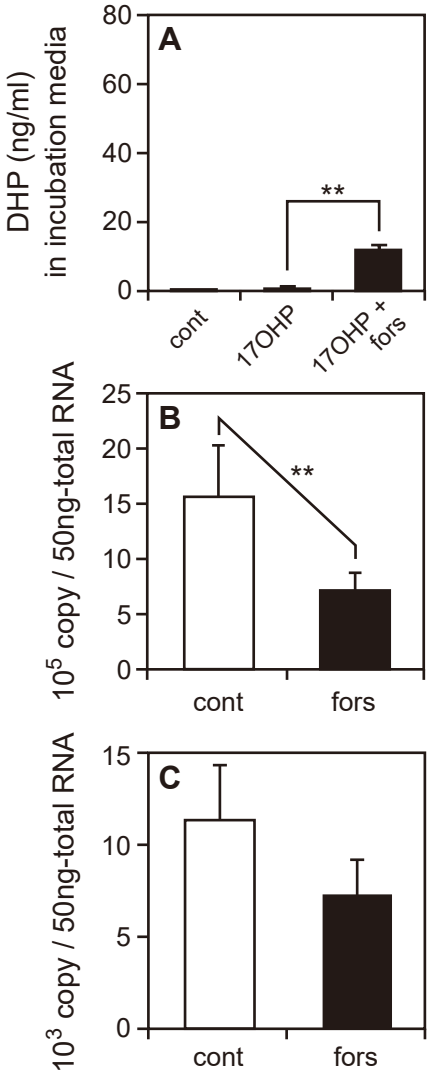

Figure 1. Production of 17α,20β-dihydroxy-4-pregnen-3-one (DHP) by isolated granulosa layers incubated in Ringer medium alone (cont), Ringer medium with 100 ng/mL 17α-hydroxyprogesterone (17OHP), or Ringer medium with 100 ng/mL 17OHP and 10 μM forskolin. Each vertical bar represents the mean ± SE of three replicate incubations from five females (total 15 incubations) (A). The raw mRNA levels of CR/20β-HSD typeA (B) and typeB (C) in granulosa layers (n = 5) incubated in Ringer medium alone or in Ringer medium with forskolin. The double asterisk indicates a significant difference of $P < .01$.

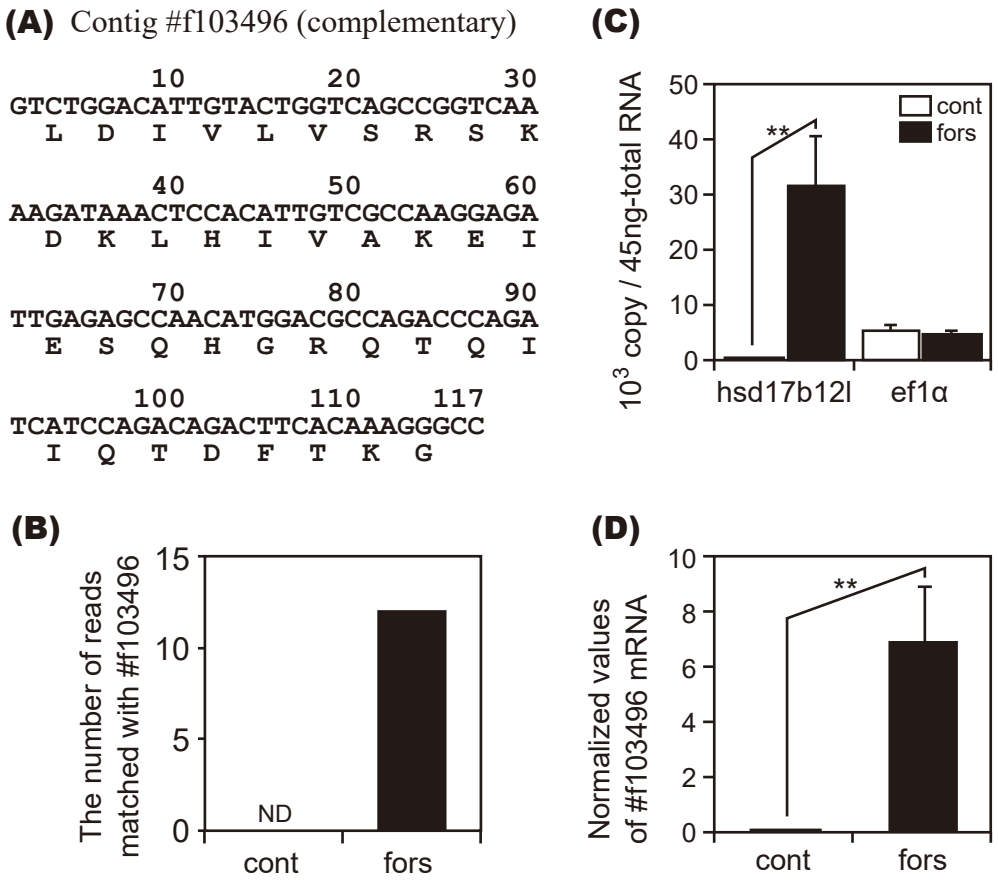

Figure 2. Sequence and expression of contig #f103496. Nucleotide and predicted amino acid sequences of contig #f103496, which encodes an amino acid sequence similar to hsd17β type 12 (A). The number of reads mapped to contig #f103496 from control (Cont) and forskolin-treated (Fors) groups. ND, not detected (B). The raw levels of #f103496 and ef1α mRNA in 45 ng of total RNA. Open and closed bars represent levels in the control or forskolin-treated groups, respectively (C). ef1α-Normalized #103496 mRNA levels (D). Each vertical bar represents the mean ± SE of five experiments using different females (B and C). The triple asterisk indicates a significant difference of $P < .0005$.

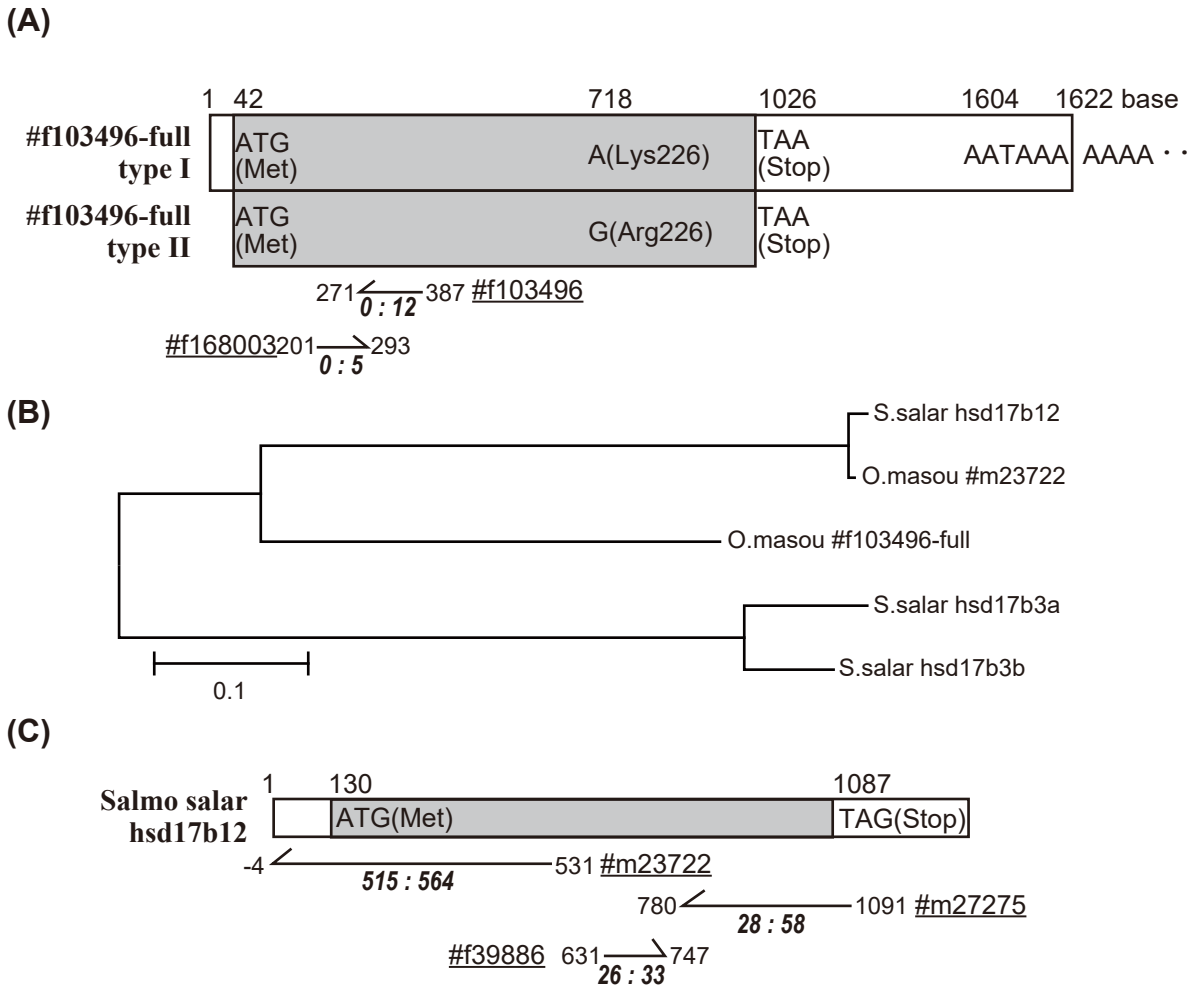

Figure 3. Schematic representation of the two coding sequence forms of full-length #103496-encoding cDNA (typeI and typeII). The closed bars represent the translated coding region and the open bars represent the 5′- and 3′-untranslated regions (A). Phylogenetic relationships were determined using predicted amino acid sequences from the masu salmon (O. masou) #f103496-full sequence; contig #m23722, which matched Salmo salar hsd17β12; S. salar hsd17β3a; and S. salar hsd17β3b (B). Schematic representation of the coding sequence of S. salar hsd17β12-encoding cDNA and matching contigs from O. masou (C). The numbers above the bars represent nucleotide positions, and the arrows underneath the bars represent the matching contigs. Right or left arrows indicate forward or reverse matching contigs, respectively. The numbers attached to arrows indicate the nucleotide position corresponding to the S. salar sequence, and underlined numbers indicate contig names. The bold italic numbers under the arrows indicate the number of mapped reads from the control and forskolin-treated groups.

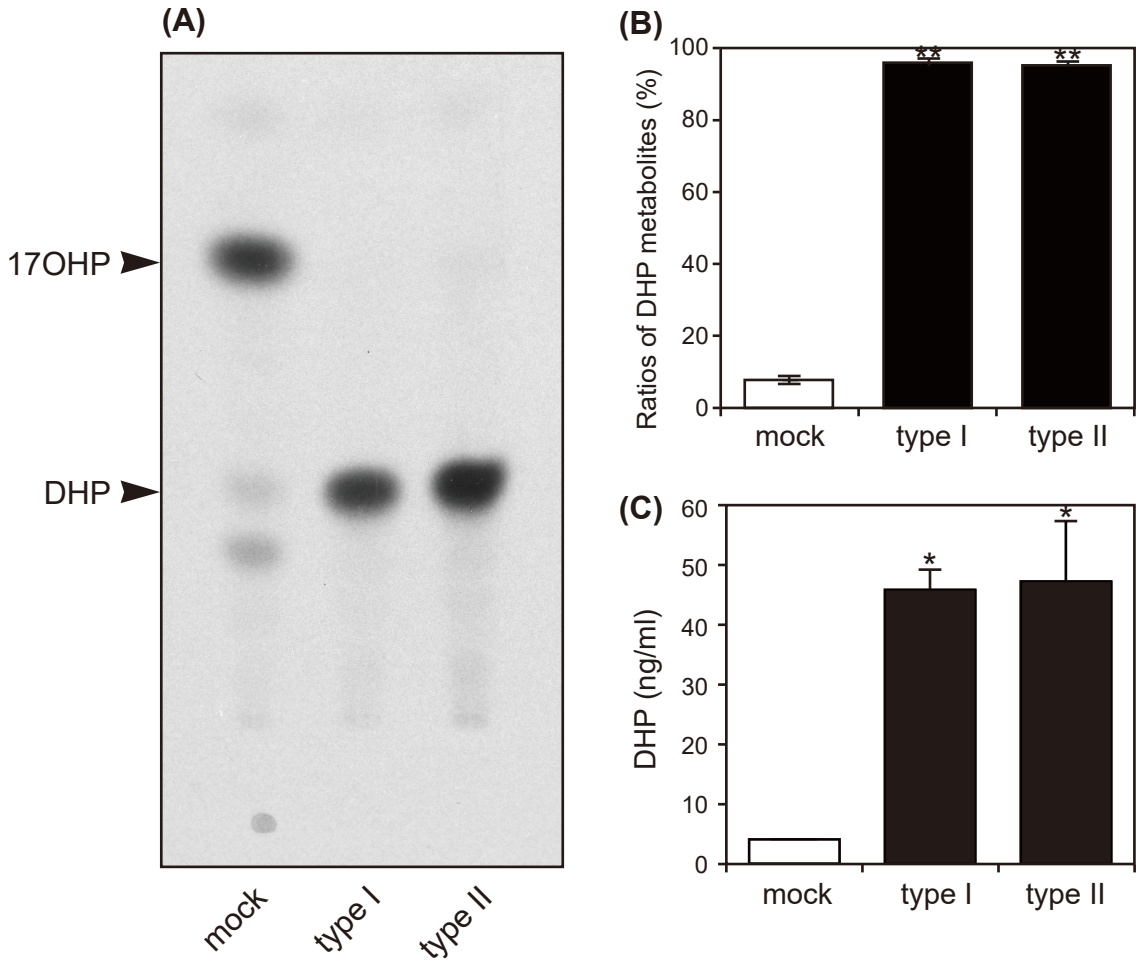

Figure 4. Enzyme activity of omhsd17β12l. Autoradiograph of thin-layer chromatography, illustrating the conversion of 3H-labeled 17α-hydroxyprogesterone (17OHP) to 17α,20 β-dihydroxy-4-pregnen-3-one (DHP) by HEK293T cells transfected with pSI containing either empty vector (mock) or omhsd17β12l typeI or typeII (A). The percent conversion of 17OHP to DHP was calculated from the autoradiograph using ImageJ (B). DHP production by HEK293T cells transfected with pSI constructs in the presence of 100 ng/mL cold 17OHP (C). In both experiments, three replicate independent transfections were conducted for each treatment. Each vertical bar represents the mean ± SE. Double and single asterisks indicate statistical differences at $P < .0001$ and $< .05$, respectively.

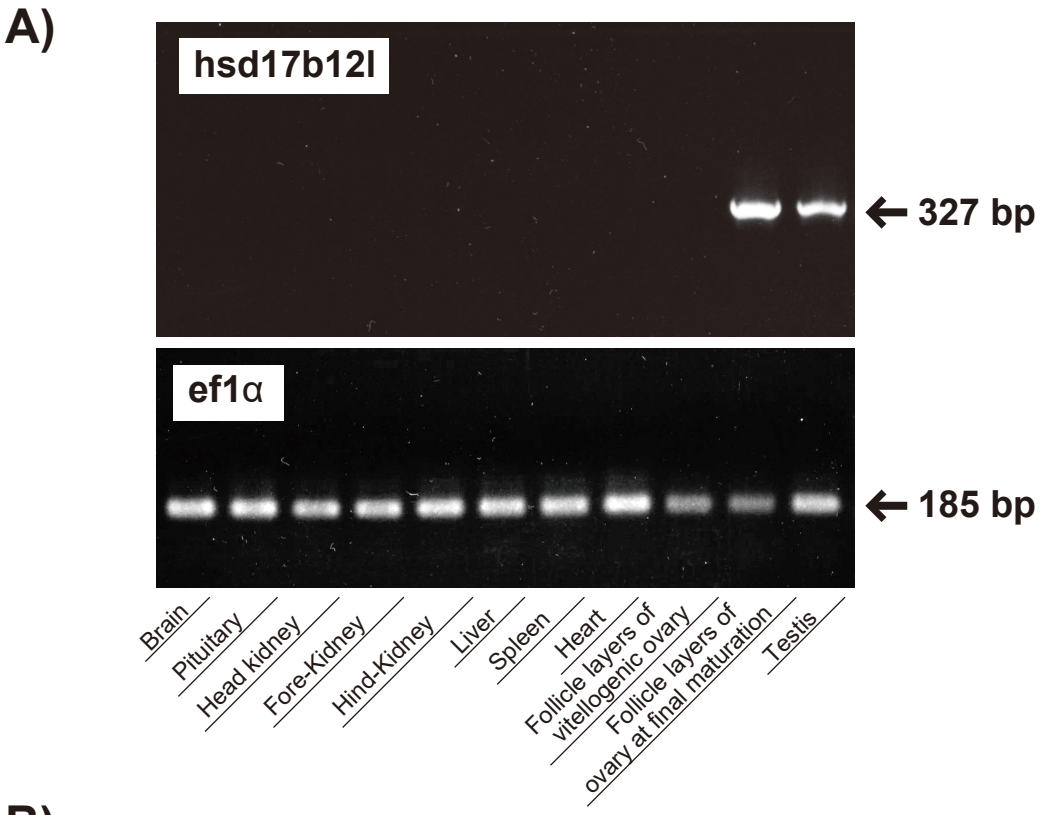

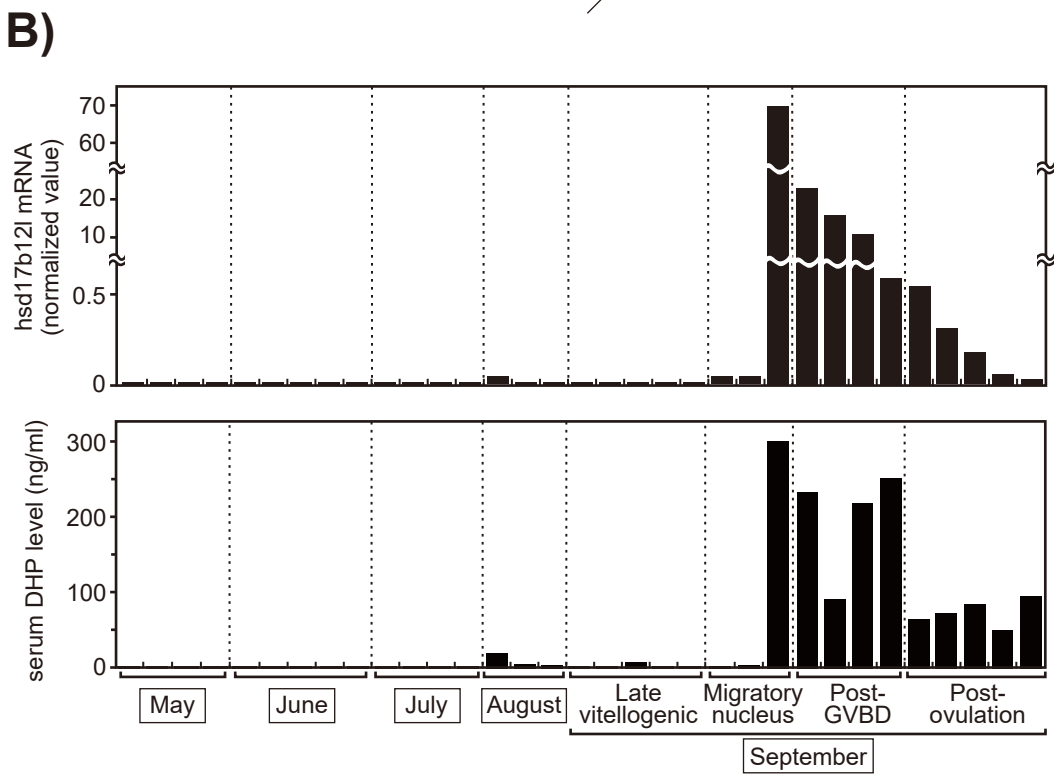

Figure 5. Tissue-specific omhsd17β12l expression and its relationship with serum DHP concentrations in ovarian follicles. Tissue-specific expression of the masu salmon (O. masou) omhsd17β12l transcript, as determined by RT-PCR. Amplification of ef1α was used as a positive control (A). Changes in serum 17α,20β-dihydroxy-4-pregnen-3-one (DHP) concentration and normalized values of omhsd17β12l in follicle layers during sexual maturation in masu salmon (B). The corresponding upper and lower column values are derived from the same fish. Migratory nucleus, follicle layers from ovaries with oocytes in which germinal vesicles were visibly close to the cell periphery. Post-GVBD, follicle layers from ovaries with oocytes after germinal vesicle breakdown. Post-ovulation, follicle layers from ovaries after ovulation.

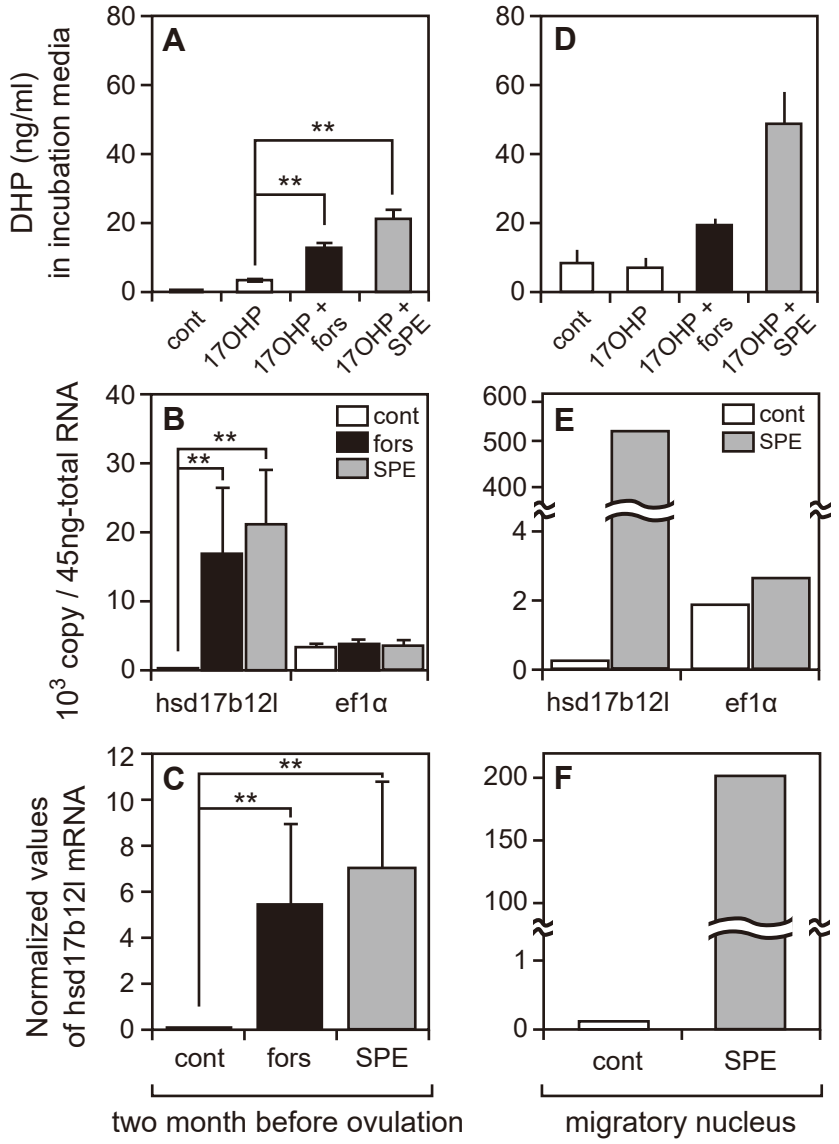

Figure 6. 20β-Hydroxysteroid dehydrogenase activity and omhsd17β12l mRNA levels in incubated granulosa layers in female masu salmon. Measurements were taken at two months before ovulation (A, B, C) and at the migratory nucleus stage (D, E, F). The concentration of 17α,20β-dihydroxy-4-pregnen-3-one (DHP) in media after incubations, that were conducted in Ringer medium alone (cont) or in Ringer medium with 100 ng/mL 17α-hydroxyprogesterone (17OHP), 17OHP and 10 μM forskolin (17OHP + fors), or 17OHP and 100 μg/mL salmon pituitary extract (17OHP + SPE) (A, D). Levels of omhsd17β12l and ef1α mRNA in 45 ng of total RNA from granulosa layers incubated in Ringer medium alone (open column), Ringer medium with forskolin (closed column), or Ringer medium with SPE (gray column) (B, E). ef1α -normalized omhsd17β12l mRNA levels (C, F). Each vertical bar represents the mean ± SE from four experiments using different females (A, B and C), or mean ± SD from single female (D). The double asterisk indicates a significant difference of $P < .01$).

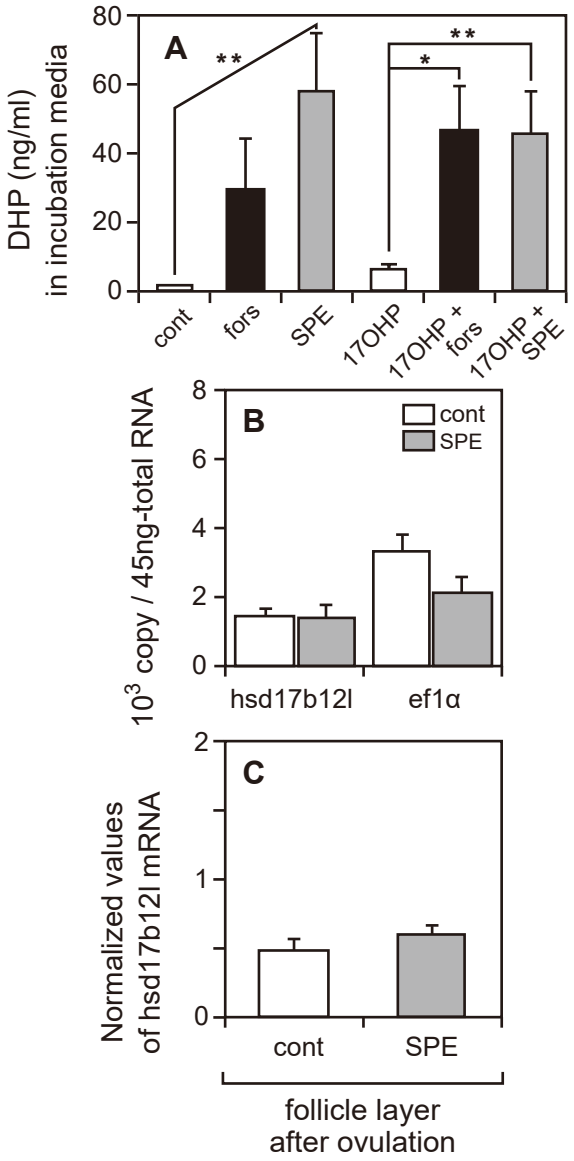

Figure 7. 17α,20β-dihydroxy-4-pregnen-3-one (DHP) production and omhsd17β12l mRNA levels in the incubated follicle layers. Incubations were conducted in Ringer medium with no additives (cont) or with 100 ng/mL 17α-hydroxyprogesterone (17OHP), 10 μM forskolin (fors), 100 μg/mL salmon pituitary extract (SPE), or a combination of 17OHP and either forskolin or SPE (A). Levels of omhsd17β12l and ef1α mRNA in 45 ng of total RNA from follicle layers incubated in Ringer medium (cont, open columns) or with SPE (gray column) (B). ef1α-Normalized omhsd17β12l mRNA levels (C). Each vertical bar represents the mean ± SE from five experiments using different females. The asterisk and double asterisk indicate significant differences of $P < .05$ and $P < .01$, respectively.

Masu salmon, *Oncorhynchus masou* ef1α partial cDNA sequence (GenBank Accession No. LC149908)

TCTGTGGAGATGCACCACGAGACCCTGGAAGCGGCTCTACCCGGTGACAATGTTGGCTTCAACGTCAAGAACGTGTCCGTCAA
GGATATCCGTCGTGGCAACGTGGCTGGAGACAGCAAGAATGACCCCCCAATGGAGGCCGGCAACTTCACAGCTCAG/GTCATC
ATCCTGAACCACCCCGGCCAGATCTCCCAGGGCTATGCCCCCGTACTGGATTGCCACACCGCTCACATCGCCTGCAAGTTCAG
CGAGCTCAAGGAGAAGATCGACCGTCGGTCCGGCAAGAAGCTTGAGGACAACCCCAAAGCCCTGAAATCTGGAGACGCCGCCA
TCATTGTCATGGTGCCAGGAAAGCCCATGTGTGTGGAGAGCTTCGCCGCCTACCCTCCCCTTG/GTCGTTTTGCCGTGCGCGA
CATGAGACAGACCGTTGCCGTTGGTGTCATCAAGGCCGTCGACAAGAAGGCTGCCAGCACTGGCAAGGTGACCAAGTCCGCCA
TTAAGGCCACCAAAGCCAAA

"/" represents predicted exon/intron boundary

ef1α 1-forward: AAATCTGGAGACGCCGCCA

ef1α 2-reverse (complementary): CCTTG/GTCGTTTTGCCGT

ef1α 3-reverse (complementary): AAGGTGACCAAGTCCGCCAT

```
         10         20         30         40         50         60
TCTGTGGAGATGCACCACGAGACCCTGGAAGCGGCTCTACCCGGTGACAATGTTGGCTTC
S  V  E  M  H  H  E  T  L  E  A  A  L  P  G  D  N  V  G  F

         70         80         90        100        110        120
AACGTCAAGAACGTGTCCGTCAAGGATATCCGTCGTGGCAACGTGGCTGGAGACAGCAAG
N  V  K  N  V  S  V  K  D  I  R  R  G  N  V  A  G  D  S  K

        130        140        150        160        170        180
AATGACCCCCCAATGGAGGCCGGCAACTTCACAGCTCAGGTCATCATCCTGAACCACCCC
N  D  P  P  M  E  A  G  N  F  T  A  Q  V  I  I  L  N  H  P

        190        200        210        220        230        240
GGCCAGATCTCCCAGGGCTATGCCCCCGTACTGGATTGCCACACCGCTCACATCGCCTGC
G  Q  I  S  Q  G  Y  A  P  V  L  D  C  H  T  A  H  I  A  C

        250        260        270        280        290        300
AAGTTCAGCGAGCTCAAGGAGAAGATCGACCGTCGGTCCGGCAAGAAGCTTGAGGACAAC
K  F  S  E  L  K  E  K  I  D  R  R  S  G  K  K  L  E  D  N

        310        320        330        340        350        360
CCCAAAGCCCTGAAATCTGGAGACGCCGCCATCATTGTCATGGTGCCAGGAAAGCCCATG
P  K  A  L  K  S  G  D  A  A  I  I  V  M  V  P  G  K  P  M

        370        380        390        400        410        420
TGTGTGGAGAGCTTCGCCGCCTACCCTCCCCTTGGTCGTTTTGCCGTGCGCGACATGAGA
C  V  E  S  F  A  A  Y  P  P  L  G  R  F  A  V  R  D  M  R

        430        440        450        460        470        480
CAGACCGTTGCCGTTGGTGTCATCAAGGCCGTCGACAAGAAGGCTGCCAGCACTGGCAAG
Q  T  V  A  V  G  V  I  K  A  V  D  K  K  A  A  S  T  G  K

        490        500        510        520
GTGACCAAGTCCGCCATTAAGGCCACCAAAGCCAAA
V  T  K  S  A  I  K  A  T  K  A  K
```

Comparison with medaka genomic sequence: ENSORLT00000002805

```
exon5           GTATTGGAACAGTCCCTGTAGGTCGCGTGGAAACTGGGGTACTAAAACCTGGCATGGTTG 60
masu            ------------------------------------------------------------

exon5           TGACCTTTGCCCCAGTCAACGTGACCACTGAAGTGAAGTCTGTGGAGATGCACCATGAGG 120
masu            ------------------------------------TCTGTGGAGATGCACCACGAGA 22
                                                    ********************* ***
```

```
exon5           CTCTAACCGAGGCTCTTCCTGGAGACAATGTGGGCTTTAATGTCAAGAATGTGTCAGTCA 180
masu            CCCTGGAAGCGGCTCTACCCGGTGACAATGTTGGCTTCAACGTCAAGAACGTGTCCGTCA 82
                * **    * ****** ** ** ******** ***** ** ******** ***** ****

exon5           AAGATATACGCCGTGGGAATGTGGCTGGCGACAGCAAGAATGACCCCCCGCAGGAAGCTG 240
masu            AGGATATCCGTCGTGGCAACGTGGCTGGAGACAGCAAGAATGACCCCCCAATGGAGGCCG 142
                * ***** ** ***** ** ******** ********************   *** ** *

exon5           CCAACTTCACTGCTCAG------------------- 257
masu            GCAACTTCACAGCTCAG------------------- 159
                 ********* ******


exon6            ----------GTGATCATTCTCAACCACCCGGGCCAGATTAGTGCAGGCTACGCTCCTGT 50
masu             ----------GTCATCATCCTGAACCACCCCGGCCAGATCTCCCAGGGCTATGCCCCCGT 209
                           ** ***** ** ******** ********       ***** ** ** **

exon6            GCTAGACTGTCACACTGCTCACATTGCCTGCAAGTTTGCAGAGCTGAAGGAAAAAATTGA 110
masu             ACTGGATTGCCACACCGCTCACATCGCCTGCAAGTTCAGCGAGCTCAAGGAGAAGATCGA 269
                  ** ** ** ***** ******** ***********    ***** ***** ** ** **

exon6            TCGTCGCTCAGGGAAGAAGCTAGAGGACAACCCCAAGTCTCTCAAGTCAGGAGATGCCGC 170
masu             CCGTCGGTCCGGCAAGAAGCTTGAGGACAACCCCAAAGCCCTGAAATCTGGAGACGCCGC 329
                  ***** ** ** ******** **************  * ** ** ** ***** *****

exon6            CATCGTAGACATGATTCCTGGGAAGCCCATGTGTGTTGAGAGCTTCTCCGAGTACCCTCC 230
masu             CATCATTGTCATGGTGCCAGGAAAGCCCATGTGTGTGGAGAGCTTCGCCGCCTACCCTCC 389
                 **** * * **** * ** ** ************** ********* ***  ********

exon6            ACTGG---------------- 235
masu             CCTTG---------------- 394
                  ** *


exon7            GTCGTTTTGCGGTTCGCGACATGCGCCAGACCGTTGCCGTTGGTGTGATAAAGGGGGTGG 60
masu             GTCGTTTTGCCGTGCGCGACATGAGACAGACCGTTGCCGTTGGTGTCATCAAGGCCGTCG 454
                 ********** ** ********* * ******************** ** ****  ** *

exon7            AGAAGAAAGTCTCCACCACTGGTAAGGTCACCAAGTCTGCTCAGAAGGCCCAGAGGAACA 120
masu             ACAAGAAGGCTGCCAGCACTGGCAAGGTGACCAAGTCCGCCATTAAGGCCACCAAAGCCA 514
                 * ***** *   *** ****** ***** ******** **    ******   *    **

exon7            AATGA 125
masu             AA--- 516
                 **
```

Masu salmon, *Oncorhynchus masou* omhsd17β12l complete cDNA sequence (GenBank Accession No. LC149904 (typeI), LC149905 (typeII))

GAAGAACTGTCTTCTGAAGTTTGAGTGAAATTTGCCCAGACATGGATACTGTATCAGACTCGATGCTTGTGAGGGGACTGGTG
TTCATAGGTGGCTTCACAGTGCTGTATTACATGCTCAAATGGTCCTGGATTTGCTGGTGTGGATTCAGAGTGTATGTGCTGTC
AAAAGTTTGGCAAACTGATTTAAAGGCATATGGACAATGGGCAG/TTGTCACAGGGGCTACCGCAGGGATTGGCAAAGCTTAC
GCAAATGAG/TTGGCCAGAAGAGGTCTGGACATTGTACTGGTCAGCCGGTCAAAAGATAAACTCCACATTGTCGCCAAGGAGA
TTG/AGAGCCAACATGGACGCCAGACCCAGATCATCCAGACAGACTTCACAAAGGGCCATGACATCTACCCTGCTATAGCTGA
GGCACTACGGGACCTGGACATAGGCATCCTGG/TTAACAATGTAGGCATGAACTATTCTGACAAGTTGGTACATTTCCTGGAC
ATTCCCAACCCTGAGCAG/AGAACCACCCAGGTGATTAACTGTAACATCCTCTCTGTCACCCAG/ATGACCAGACTGGTTCTC
CCACGCATGGTTTCAAG/AGGGAACGGTCTGATCATCAACATGTCTTCAGAGGCAGGTGCTCAACCACAACCCATGCTGTCTC
TCTACTCCGCCACCAAG/ATTTTTGTGACATATTTTTCCAGATCTCTGAATTCAGAGTACARGTCACAGGGAATAACAGTTCA
G/TGTGTGGCTCCCTTTATGGTGTCCACTAACATGACCCACAACTTGCCCCCCAACCTGTTGTTGAAGAGTGCCAGTGCTTTT
GCCCGTGAAGCTCTGAACACAGTGGGTCACTCCAGCTACACCAGCGGCTGTGTCTCTCACGCTCTTCAA/AACATTGCTCTGT
CCATTTTCTTCCCTGATTGGCTACGCCTTTCATCCTACTGTGTGAAGCAGACAGAGAAATTTGCACAGAGCATGgAGAAGAAA
ATTGATGAAATGaCAGAACGTTCTGCAAGCAAAGAGGACTAAGGAGTGCAAAGGAGGTTGTTACTGAAACGTTGGTGGTGCTT
TAAAGAGGTCATATTGGAAATTGAAACGAGTTTTACTTCATATGTAGAGAACTAATTGATCGATGTTACTGTTTTTGCATTGA
CTGCCATTGAAAGGTATTGGTAATAGGAAAGAGATTGTGTAAAGTTGATGTGATGTAAACAAGCTGACCCCAAATCCATCATG
AACTATATAGCCTGAGTGCAGCAGAGTATGATCTGTGGGAGACTCTCAAACAGGCTTCTATAGTACATATGTTAGCTATATAC
TTATTAGGGATATAGACTACAACATAACTGAATGCTTGAACATATGCATGTTCTGGTTGATTTGGACTTTTAACATAGTACAA
TTTTTGGCATCAACATTTACATTTACATTTAAGTCATTTAGCAGACGCTCTTATCCAGAGCGACTTACAAATTGGTGAATTCA
CCTTCTGACATCCAGTGGAACAGCCACTTTACAATAGTGCATCTAAATCATTTAAGGAGGGGGGGGGGTGAGAAGGATTACTT
ATCCTATCACATTTTTGTGATTTCGATTTTCTTAGAAATAAATAGAAAGGCAATCAAAAAAAAAAAAAAAAAAAAA

"/" represents predicted exon/intron boundary

omhsd17β12l 1-forward: GAGTGAAATTTGCCCAGACATGG
omhsd17β12l 2-reverse (complementary): GATTG/AGAGCCAACATGGACG
omhsd17β12l 3-forward: ATGGACAATGGGCAG/TTGTCA
omhsd17β12l 4-reverse (complementary): TACGCAAATGAG/TTGGCCAGAA

```
         10        20        30        40        50        60
GAAGAACTGTCTTCTGAAGTTTGAGTGAAATTTGCCCAGACATGGATACTGTATCAGACT
                                          M  D  T  V  S  D  S

         70        80        90       100       110       120
CGATGCTTGTGAGGGGACTGGTGTTCATAGGTGGCTTCACAGTGCTGTATTACATGCTCA
  M  L  V  R  G  L  V  F  I  G  G  F  T  V  L  Y  Y  M  L  K

       130       140       150       160       170       180
AATGGTCCTGGATTTGCTGGTGTGGATTCAGAGTGTATGTGCTGTCAAAAGTTTGGCAAA
  W  S  W  I  C  W  C  G  F  R  V  Y  V  L  S  K  V  W  Q  T

       190       200       210       220       230       240
CTGATTTAAAGGCATATGGACAATGGGCAGTTGTCACAGGGGCTACCGCAGGGATTGGCA
  D  L  K  A  Y  G  Q  W  A  V  V  T  G  A  T  A  G  I  G  K

       250       260       270       280       290       300
AAGCTTACGCAAATGAGTTGGCCAGAAGAGGTCTGGACATTGTACTGGTCAGCCGGTCAA
  A  Y  A  N  E  L  A  R  R  G  L  D  I  V  L  V  S  R  S  K

       310       320       330       340       350       360
AAGATAAACTCCACATTGTCGCCAAGGAGATTGAGAGCCAACATGGACGCCGGACCCAGA
  D  K  L  H  I  V  A  K  E  I  E  S  Q  H  G  R  R  T  Q  I

       370       380       390       400       410       420
TCATCCAGACAGACTTCACAAAGGGCCATGACATCTACCCTGCTATAGCTGAGGCACTAC
  I  Q  T  D  F  T  K  G  H  D  I  Y  P  A  I  A  E  A  L  R

       430       440       450       460       470       480
GGGACCTGGACATAGGCATCCTGGTTAACAATGTAGGCATGAACTATTCTGACAAGTTGG
  D  L  D  I  G  I  L  V  N  N  V  G  M  N  Y  S  D  K  L  V
```

```
       490       500       510       520       530       540
TACATTTCCTGGACATTCCCAACCCTGAGCAGAGAACCACCCAGGTGATTAACTGTAACA
  H  F  L  D  I  P  N  P  E  Q  R  T  T  Q  V  I  N  C  N  I

       550       560       570       580       590       600
TCCTCTCTGTCACCCAGATGACCAGACTGGTTCTCCCACGCATGGTTTCAAGAGGGAACG
  L  S  V  T  Q  M  T  R  L  V  L  P  R  M  V  S  R  G  N  G

       610       620       630       640       650       660
GTCTGATCATCAACATGTCTTCAGAGGCAGGTGCTCAACCACAACCCATGCTGTCTCTCT
  L  I  I  N  M  S  S  E  A  G  A  Q  P  Q  P  M  L  S  L  Y

       670       680       690       700       710       720
ACTCCGCCACCAAGATTTTTGTGACATATTTTTCCAGATCTCTGAATTCAGAGTACARGT
  S  A  T  K  I  F  V  T  Y  F  S  R  S  L  N  S  E  Y  #  S

       730       740       750       760       770       780
CACAGGGAATAACAGTTCAGTGTGTGGCTCCCTTTATGGTGTCCACTAACATGACCCACA
  Q  G  I  T  V  Q  C  V  A  P  F  M  V  S  T  N  M  T  H  N

       790       800       810       820       830       840
ACTTGCCCCCCAACCTGTTGTTGAAGAGTGCCAGTGCTTTTGCCCGTGAAGCTCTGAACA
  L  P  P  N  L  L  L  K  S  A  S  A  F  A  R  E  A  L  N  T

       850       860       870       880       890       900
CAGTGGGTCACTCCAGCTACACCAGCGGCTGTGTCTCTCACGCTCTTCAAAACATTGCTC
  V  G  H  S  S  Y  T  S  G  C  V  S  H  A  L  Q  N  I  A  L

       910       920       930       940       950       960
TGTCCATTTTCTTCCCTGATTGGCTACGCCTTTCATCCTACTGTGTGAAGCAGACAGAGA
  S  I  F  F  P  D  W  L  R  L  S  S  Y  C  V  K  Q  T  E  K

       970       980       990      1000      1010      1020
AATTTGCACAGAGCATGgAGAAGAAAATTGATGAAATGGCAGAACGTTCTGCAAGCAAAG
  F  A  Q  S  M  E  K  K  I  D  E  M  A  E  R  S  A  S  K  E

      1030      1040      1050      1060      1070      1080
AGGACTAAGGAGTGCAAAGGAGGTTGTTACTGAAACGTTGGTGGTGCTTTAAAGAGGTCA
  D  *

      1090      1100      1110      1120      1130      1140
TATTGGAAATTGAAACGAGTTTTACTTCATATGTAGAGAACTAATTGATCGATGTTACTG

      1150      1160      1170      1180      1190      1200
TTTTTGCATTGACTGCCATTGAAAGGTATTGGTAATAGGAAAGAGATTGTGTAAAGTTGA

      1210      1220      1230      1240      1250      1260
TGTGATGTAAACAAGCTGACCCCAAATCCATCATGAACTATATAGCCTGAGTGCAGCAGA

      1270      1280      1290      1300      1310      1320
GTATGATCTGTGGGAGACTCTCAAACAGGCTTCTATAGTACATATGTTAGCTATATACTT

      1330      1340      1350      1360      1370      1380
ATTAGGGATATAGACTACAACATAACTGAATGCTTGAACATATGCATGTTCTGGTTGATT

      1390      1400      1410      1420      1430      1440
TGGACTTTTAACATAGTACAATTTTTGGCATCAACATTTACATTTACATTTAAGTCATTT

      1450      1460      1470      1480      1490      1500
AGCAGACGCTCTTATCCAGAGCGACTTACAAATTGGTGAATTCACCTTCTGACATCCAGT

      1510      1520      1530      1540      1550      1560
GGAACAGCCACTTTACAATAGTGCATCTAAATCATTTAAGGAGGGGGGGGGGTGAGAAGG

      1570      1580      1590      1600      1610      1620
ATTACTTATCCTATCACATTTTTGTGATTTCGATTTTCTTAGAAATAAATAGAAAGGCAA

      1630      1640      1650
TCAAAAAAAAAAAAAAAAAAAA
```

#: K or R

Comparison with medaka genomic sequence: ENSORLT00000009884

```
medaka_exon1      ----------ATGTGGTTC-ATTCCTGTT------TTGGCCATCTTTGGAGGGATAACG 42
masu           42 ATGGATACTGTATCAGACTCGATGCTTGTGAGGGGACTGGTGTTCATAGGTGGCTTCACA 101
                     **  *  ** ** * ***        ***   ** * ** **  * **

medaka_exon1      ATTGTCTTTTACCTGCTGAAATTCACCTGGAAATGTTGGTGTGGATTCAAAGAGTTTGTC 102
masu              GTGCTGTATTACATGCTCAAATGGTCCTGGATTTGCTGGTGTGGATTCAGAGTGTATGTG 161
                   *  * * **** **** ****   ******  ** ************ ** ** ***

medaka_exon1      TTGTCGGAGTATTGGCCAGTGAACTTAAAGAAATATGGAACATGGGCAG 151
masu              CTGTCAAAAGTTTGGCAAACTGATTTAAAGGCATATGGACAATGGGCAG 210
                   ****  *   ***** *    * ******  *******  ********


medaka_exon2      TTGTCACCGGAGCCACATCTGGTATTGGCAAAGCTTACGCCACTGAG 47
masu           211 TTGTCACAGGGGCTACCGCAGGGATTGGCAAAGCTTACGCAAATGAG 257
                   ******* ** ** **  * ** ***************** * ****


medaka_exon3      CTTGCACGCAGAGGTCTGGATGTTATCTTGATTGGCAGATCTGATGATAAACTGCAAACG 60
masu           258 TTGGCCAGAAGAGGTCTGGACATTGTACTGGTCAGCCGGTCAAAAGATAAACTCCACATT 60
                   * **  * ***********  ** *  ** *  ** * **  * ******** ** *

medaka_exon3      GTTGCCAAGGAGATCG 76
masu              GTCGCCAAGGAGATTG 333
                  ** ********** *


medaka_exon4      AAAAGGAGTTTGGACAGAAGACTCGCACCATCCGAGTGGACTTCACAGACGGCTGCAGCA 60
masu           334 AGAGCCAACATGGACGCCAGACCCAGATCATCCAGACAGACTTCACAAAGGGCCATGACA 393
                   * *   *   *****   **** *  * *****     ********* * ***     **

medaka_exon4      TCTATTCTACCATTGCCAAAGAACTTCAAGATCTGGAGATTGGAATATTAG 111
masu              TCTACCCTGCTATAGCTGAGGCACTACGGGACCTGGACATAGGCATCCTGG 444
                  ****  ** * ** **  * * *** *  ** ***** ** ** **  * *
```

Masu salmon, *Oncorhynchus masou CR/20β-HSD typeA* partial cDNA sequence (GenBank Accession No. LC149906)

AAAGTGGCAGTAGTTACCGGTGCCAATAAAGGCATAGGACTTGCGATTGTGAGGGAGCTTTGTAAGGCAAAATTTACCGGGGA
TGTTATTCTTACTGCTCGAAATGAGAAACTTGGAAATGAGGCAGTGAAGATGCTGAAGTCTGAAGGATTTGAAGTTGCTTTCC
ACCACCTTGATATCTGCGACCAGGGCAGCGCCAAGCAACTGAGTAACTTTCTGCAGAAGACATATGGGGGATTGGATGTGCTC
ATTAACAACGCGGGAATGGCTTTTAAGAATGACGCGACTGAGACTTTTGGGGAACAGGCTGAGGTGACCATGCGCACCAACTT
TTGGGGCACCCTGTGGGTGTGCCATGCTCTCCTACCCCTCCTCAGACCAAATGCCAGAGTGGTGAATGTCTCCAGCTTTGTTA
GCAAGAAGGCTCTTGATACATGCAGCCCTCAACTACAAGCCAAGTTCCGTGATACTGAGCTCTCTGAGGAGGAGCTGTGCTTG
CTGATGGGGCAGTTTGTTATTGCCGCTCAGCAGGGAAACCATCAGGCCCAGGGGTGGCCAAACACAGCCTATGGCACAACAAA
GATCGGAGTGACTGTGCTGTCCAGGATTCAGGCTAATTTTCTGACTAAGACCCGGGCAGCTGATGGAATCCTGCTCAACGCCT
GCTGCCCTGGCTGGGT

CR/20β-HSD typeA forward: CCGGTGCCAATAAAGGCAT
CR/20β-HSD typeA reverse (complementary): CTTGCGATTGTGAGGGAGCT

```
         10        20        30        40        50        60
AAAGTGGCAGTAGTTACCGGTGCCAATAAAGGCATAGGACTTGCGATTGTGAGGGAGCTT
K  V  A  V  V  T  G  A  N  K  G  I  G  L  A  I  V  R  E  L

         70        80        90       100       110       120
TGTAAGGCAAAATTTACCGGGGATGTTATTCTTACTGCTCGAAATGAGAAACTTGGAAAT
C  K  A  K  F  T  G  D  V  I  L  T  A  R  N  E  K  L  G  N

        130       140       150       160       170       180
GAGGCAGTGAAGATGCTGAAGTCTGAAGGATTTGAAGTTGCTTTCCACCACCTTGATATC
E  A  V  K  M  L  K  S  E  G  F  E  V  A  F  H  H  L  D  I

        190       200       210       220       230       240
TGCGACCAGGGCAGCGCCAAGCAACTGAGTAACTTTCTGCAGAAGACATATGGGGGATTG
C  D  Q  G  S  A  K  Q  L  S  N  F  L  Q  K  T  Y  G  G  L

        250       260       270       280       290       300
GATGTGCTCATTAACAACGCGGGAATGGCTTTTAAGAATGACGCGACTGAGACTTTTGGG
D  V  L  I  N  N  A  G  M  A  F  K  N  D  A  T  E  T  F  G

        310       320       330       340       350       360
GAACAGGCTGAGGTGACCATGCGCACCAACTTTTGGGGCACCCTGTGGGTGTGCCATGCT
E  Q  A  E  V  T  M  R  T  N  F  W  G  T  L  W  V  C  H  A

        370       380       390       400       410       420
CTCCTACCCCTCCTCAGACCAAATGCCAGAGTGGTGAATGTCTCCAGCTTTGTTAGCAAG
L  L  P  L  L  R  P  N  A  R  V  V  N  V  S  S  F  V  S  K

        430       440       450       460       470       480
AAGGCTCTTGATACATGCAGCCCTCAACTACAAGCCAAGTTCCGTGATACTGAGCTCTCT
K  A  L  D  T  C  S  P  Q  L  Q  A  K  F  R  D  T  E  L  S

        490       500       510       520       530       540
GAGGAGGAGCTGTGCTTGCTGATGGGGCAGTTTGTTATTGCCGCTCAGCAGGGAAACCAT
E  E  E  L  C  L  L  M  G  Q  F  V  I  A  A  Q  Q  G  N  H

        550       560       570       580       590       600
CAGGCCCAGGGGTGGCCAAACACAGCCTATGGCACAACAAAGATCGGAGTGACTGTGCTG
Q  A  Q  G  W  P  N  T  A  Y  G  T  T  K  I  G  V  T  V  L

        610       620       630       640       650       660
TCCAGGATTCAGGCTAATTTTCTGACTAAGACCCGGGCAGCTGATGGAATCCTGCTCAAC
S  R  I  Q  A  N  F  L  T  K  T  R  A  A  D  G  I  L  L  N

        670       680
GCCTGCTGCCCTGGCTGGGT
A  C  C  P  G  W
```

Masu salmon, *Oncorhynchus masou CR/20β-HSD typeB* partial cDNA sequence (GenBank Accession No. LC149907)

AAAGTGGCAGTAGTTACCGGTGCCAATAAAGGCACAGGATTTGCGATTGTGAGGGAGCTTTGTAAGGCAAAATTTACCGGGGA
TGTTATTCTTACTGCTCGAAATGAGAAACTTGGAAATGAGGCAGTGAAGATGCTGAAGTCTGAAGGATTTGAAGTTGCTTTCC
ACCACCTTGATATCTGCGACCAGGGCAGCGCCAAGCAACTGAGTAACTTTCTGCAGAAGACATATGGGGGATTGGATGTGCTC
ATTAACAACGCTGGAATGTCCTTTAAAAATGATGCGACTGAGACTTTTGGGGAACAGGCTGAGGTGACCATGCGCACCAACTT
TTGGGGCACCCTGTGGGTGTGCCATGCTCTCCTACCCCTCCTCAGACCAAATGCCAGAGTGGTGAATGTCTCCAGCTTTGTTA
GCAAGAAAGCTCTTGATACATGCAGCCCTCAACTACAAGCCAAGTTCCGGGATACTGAGCTCTCTGAGGAGGAGCTGTGCTTG
CTGATGGGGCAGTTTGTTATTGCCGCTCAGCAGGGAAACCATCAGGCCCAGGGGTGGCCAAACACAGCCTATGGCACAACAAA
GATCGGAGTGACTGTGTTGTCCAGGATTCAGGCTCATTTTCTGACTAAGACCCGGGCAGCTGATGGAATCCTGCTCAACGCCT
GCTGCCCTGGCTGGGT

CR/20β-HSD typeB forward: TCATTAACAACGCTGGAATGTCC
CR/20β-HSD typeB reverse (complementary): AAAATGATGCGACTGAGACTTTTGG

```
         10        20        30        40        50        60
AAAGTGGCAGTAGTTACCGGTGCCAATAAAGGCACAGGATTTGCGATTGTGAGGGAGCTT
K  V  A  V  V  T  G  A  N  K  G  T  G  F  A  I  V  R  E  L

         70        80        90       100       110       120
TGTAAGGCAAAATTTACCGGGGATGTTATTCTTACTGCTCGAAATGAGAAACTTGGAAAT
C  K  A  K  F  T  G  D  V  I  L  T  A  R  N  E  K  L  G  N

        130       140       150       160       170       180
GAGGCAGTGAAGATGCTGAAGTCTGAAGGATTTGAAGTTGCTTTCCACCACCTTGATATC
E  A  V  K  M  L  K  S  E  G  F  E  V  A  F  H  H  L  D  I

        190       200       210       220       230       240
TGCGACCAGGGCAGCGCCAAGCAACTGAGTAACTTTCTGCAGAAGACATATGGGGGATTG
C  D  Q  G  S  A  K  Q  L  S  N  F  L  Q  K  T  Y  G  G  L

        250       260       270       280       290       300
GATGTGCTCATTAACAACGCTGGAATGTCCTTTAAAAATGATGCGACTGAGACTTTTGGG
D  V  L  I  N  N  A  G  M  S  F  K  N  D  A  T  E  T  F  G

        310       320       330       340       350       360
GAACAGGCTGAGGTGACCATGCGCACCAACTTTTGGGGCACCCTGTGGGTGTGCCATGCT
E  Q  A  E  V  T  M  R  T  N  F  W  G  T  L  W  V  C  H  A

        370       380       390       400       410       420
CTCCTACCCCTCCTCAGACCAAATGCCAGAGTGGTGAATGTCTCCAGCTTTGTTAGCAAG
L  L  P  L  L  R  P  N  A  R  V  V  N  V  S  S  F  V  S  K

        430       440       450       460       470       480
AAAGCTCTTGATACATGCAGCCCTCAACTACAAGCCAAGTTCCGGGATACTGAGCTCTCT
K  A  L  D  T  C  S  P  Q  L  Q  A  K  F  R  D  T  E  L  S

        490       500       510       520       530       540
GAGGAGGAGCTGTGCTTGCTGATGGGGCAGTTTGTTATTGCCGCTCAGCAGGGAAACCAT
E  E  E  L  C  L  L  M  G  Q  F  V  I  A  A  Q  Q  G  N  H

        550       560       570       580       590       600
CAGGCCCAGGGGTGGCCAAACACAGCCTATGGCACAACAAAGATCGGAGTGACTGTGTTG
Q  A  Q  G  W  P  N  T  A  Y  G  T  T  K  I  G  V  T  V  L

        610       620       630       640       650       660
TCCAGGATTCAGGCTCATTTTCTGACTAAGACCCGGGCAGCTGATGGAATCCTGCTCAAC
S  R  I  Q  A  H  F  L  T  K  T  R  A  A  D  G  I  L  L  N

        670       680
GCCTGCTGCCCTGGCTGGGT
A  C  C  P  G  W
```

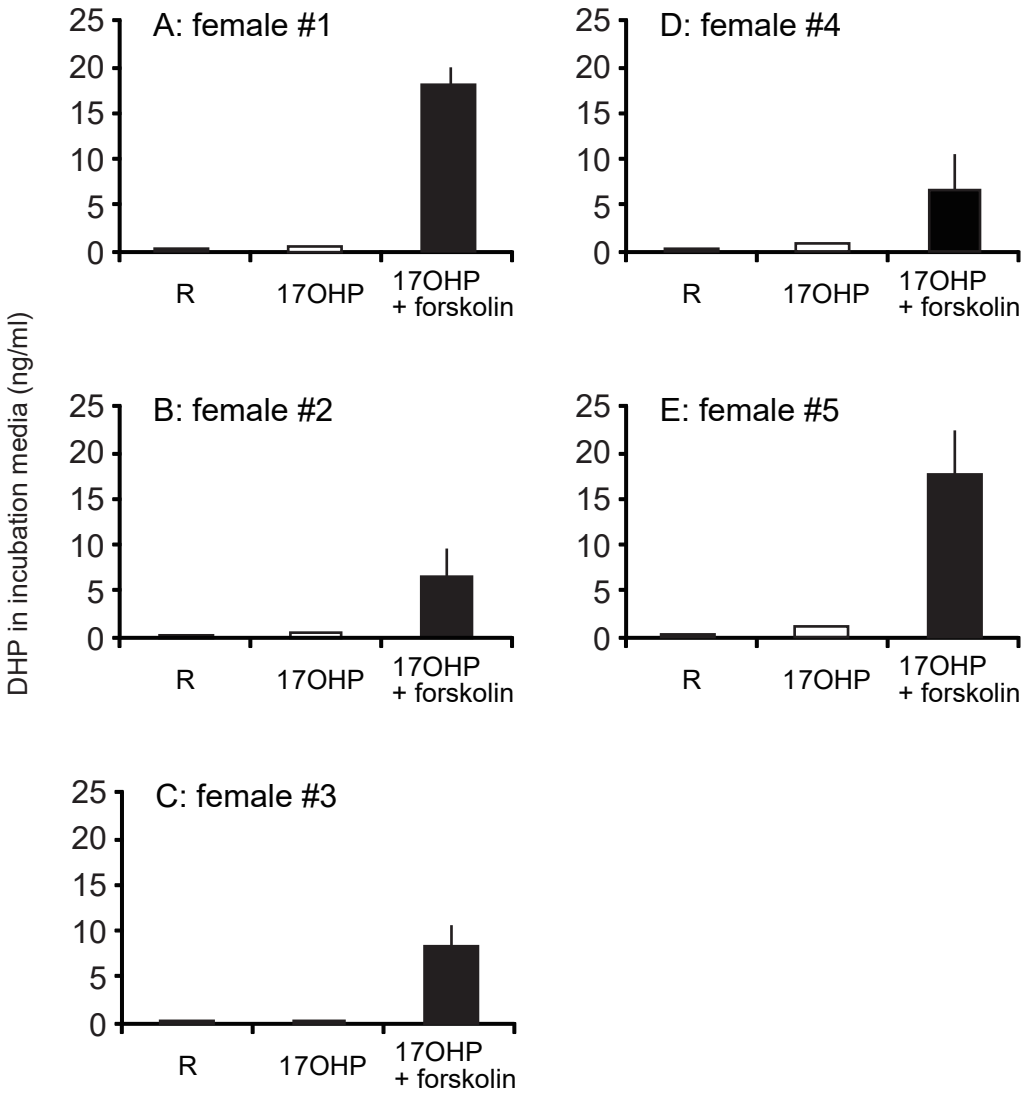

Suppemental fig. 2

cDNA#: 0503I

Predicted mevalonate (diphospho) decarboxylase:

ATAGTAGACAGTCTCGCGTTTCTAGTAATTTTTGTTATTTTATTGATACGGGTTTGACTTTTTATCAAAATGCCCGAGGACAG
CGTCAAAGAGCTCACCATGGTAACATGCAGTGCGCCTGTGAATATTGCTGTTATCAAATACTGGGGGAAGAGGGATGAGGAGT
TGATTCTACCTATAAATTCATCTTTGAGTGCCACATTACATCAAGACCAGCTCAAGACGACCACAACAGTGGCATGCAGCAGG
TCGTTCCAGGAGGATCGTATCTGGCTCAACGGCAAAGAGGAGGACATAACCCAGCCCAGACTACAGTCCTGCCTTAGGGAGAG
TCAGTTACTATATGCAATGATATGATGGAGGGAGAGGGGGAAGAGTAAGAGGGCAAAGGACAAGCCATGATGTGTTGTTGTTG
GTTTCCTTACTTAGTTCGGCGCCTGGCCCGTAAGCGACGTAGTGATGGGGTGGCTGTACATAAGAGGGACTTTACTGCGTTCG
CTGAGCTGACCATGAAGGATAGCAATCAGTTCCATGCCACTTGCCTGGACACCTACCCACCCATCTTCTACCTCAACGACGTG
TCGCGCCGTGTTATCAACCTTGTGCACCGCTATAACCGTCACTACAGGGAAACAAAGGTGGCATACACATTTGATGCACGTCC
CAATGCAGTGATCTACACTCTTCAGCAGAATGTGGAAGAGTTTGTCCAGGTGGTCAAACACTTCTTCCCACCAGAGACCAATG
GAGGACAGTTTCTAAAGGGTCTTCCGGTTGCCCCAACA

qPCR primer set:

0503I_1F-forward: CGTATCTGGCTCAACGGCA

0503I_2R-reverse: CCCCCTCTCCCTCCATCAT

cDNA#: 0414B

Uunknown

GAtGTATCTTTAGATAGATTTGGCACTTACAAACTGTAGAGTTTGTGCTTATTTTGAGAACAATAGGATGATAACCCACAGAA
GGGTAACTAGAGATTTACGTGACAGAGATACCAAACCAAAAGGCCCCCGGACAGTGTAATTCACTGTATCTTTGGGTCAGCAT
TAAAACCATCCATGCCTGAAAATCTGCTAGGTAGATCTTCCCTTATAGGTCTCCATGACTGGTTTTCAGATATCACCAATCCT
CCCTCCATTGTTCCCTTAGGTTTACTGACATACTCAAAGGTACTTCAACTGCCTTATTGACTATACCCTCACTCCAGCAGACT
TACATGGCAATCGTGTGTGTCAGTGAGTGTGTGTGTGCGTGTGCGTGTACGAGTATCAGAAAGTGTGTTTGTGAGAGTGAGTG
TGTGTGCGTCCGTGTAGCCTTTGCCACCTGGCCTGACCGGACTCCACACTCCTATTCCTGTTTGTCACTAGAGCTCAAGTTGG
TCCTTTGCTGTTTATAACAGTGTATTTATTACTTTCAGCTGTACATAAGAATACTGTTTCAGTCAGTGTAAATCTATTTAAAT
GTATATGCACTTGCATTACCTGGAAGTTGGTGGTGTCTAGCGTGTTCAAGGCTCTGCGTCGGAGTCTTTTTTTAGATTCGTTA
TTATGATATTGTTTCCTTTTTTTTTTAAATATATTATATCCTAAGTAAATATATTCACACAAATGTTTGAGTGCCCTGAGCAA
CAGCTAACGAGACATATACACAACCTGTAGGTTGACAA

qPCR primer set:

0414B_1F-forward: ATCCTCCCTCCATTGTTCCCT

0414B_2R-reverse: CTGACACACACGATTGCCATG

cDNA#: 0509L

Predicted cAMP-dependent protein kinase catalytic subunit beta:

GGTGGTGACAGGATTTGGACTCCTTCTTTCATATTTGGCTGTAACGTTATCAATTGAATTTCTCTATATTGTTCCAAATTAAC
GATTTTGCCTACAAGGGGAACGTCACTCAACAACAGCTGTAGCTAGCTACCGCCATCTCCCGCAGTCTGAGCGATCGCCGTGT
CTTCCATAAGATGGGAAACGCTGCTACCGCCAAGAAAGGCAACGAGCTGGAGAGCGTGAAAGAGTTCCTAGCCAAAGCCAAAG
AAGACTTCTTACGGAAATGGGAATGTCCACCACAGACCACGACGGGCCTAGATGACTTTGACGGGCTAAAGACCCTGGGTACA
GGCTCATTTGGAAGAGTCATGCCGGTCAAACATAAAGGAACCGAGCAGTTCTTCGCCATGAAAATACTGGACAAGCAAAAGGT

GGTGAAACTCGAGCAAATAGAACACACGTTAAATGAGAAGAGAATATTGCAGGCCGTGTCTTTTCCCTTCCTCGTCAGACTTG
ATTATGCCTTCAAGGACAACTCCAATTTGTACATGGTGATGGAGTATGTTCCAGGAGGAGAGATGTTTTCGCATCTAAGACGA
ATCGGAAGGTTCAGTGAACCCCACGCACGGTTTTACGCGGCCCAGATAGTGCTGACATTTGAGTACCTCCGTTCACTAGACCT
TATCTACAGAGATCTGAAGCCTGAGAACCTTCTAATCGATCAGCATGGCTACATCCAGGTGACAGACTTTGGATTTGCCAAGA
GGGTAAAAGGCAGAACCCTGGACGTTGTGTGAACTCCAGAGTACCTGGCGCCCGAGAT

qPCR primer set:

0509L_1F-forward: GAAAGGCAACGAGCTGGAGAG

0509L_2R-reverse: TCTAGGCCCGTCGTGGTCT

cDNA#: 0408O

Predicted CREB cAMP responsive element modulator:

TTTCTGTTAGAGAGCTGAGATAAAGGGTTTCTATTGGACCTCTTAAGAACCGATATGGCTGTTGCTGGGGATGAGACTGAGTC
AGCTTCCACTGGTGACATGTCAGGCTACCAGATCTGCACTCCCACCTCCAGCCTGCCCCAGGGCGTTGTGATGGCTGGCTCCC
CAGGCTCCCTGCACAGCCCCCCCCCACGTGGCTGACGAGACCACACGCAAGAGACAACTCCGCCTCATGAAGAACAGGCAGGC
AGCCAAAGAGTGCCGGCGGAGGAAGAGAGAGTATATTCGCTGTCTGGAGACTCGCCTCACCATGCTGGAGGCCCAGAACAAGA
AGCTCATGGATGAGCTAAACTACTTTAAGGAAATGTATGGAATTAAGTCGAGTCAGTAACAGTACAGCATACTGTACATACAC
ACCCTGTAGAGACATGTTATTTATGTCTATCATAACCAGCTACTGTACATAACATTGCACAGTAATGTGTTTATTTTCAATAA
AATATGCCATATGGTTGTATGGCATTCGCTTTTAAATTGTTTTAAACATTCTCATCGAAGATCTGTTATTTGAAGATTTATCA
GACAAAATGCTCCCAGAGGTTTATCTTGAATGACATGTGGAGTCTCAGGCCTGCACATATAGCAATGTATAGGCATTATTTTG
TAGAGACTAGGGCTTGCATAGAGACCTCTGTCTTAAATGACATTTTACAAAGAAACGAACCAGCAT

qPCR primer set:

0408O_1F-forward: AAGAACAGGCAGGCAGCCA

0408O_2R-reverse: TGAGCTTCTTGTTCTGGGCC

cDNA#: 0510B

Predicted phosphatase, orphan 1:

CAGATGCGGTAGCCGGGCACCACCAACCACTCAGGACGAGGGGCACAGAGCCGACCATTTGAAAACACATGTTCACCGGTGTG
GGCGAGCCACCGCTCCACCGCTCCTCAAACATGGCTGCCTCATCTGTCCCTTCCACGGCCCCAGTCCCGTCCCCTCCCAAACG
CTTCCTGGTTCTCTTTGACTTTGACGAGACTATCGTCAACGAGAGCAGCGACGATGCAGTGGTGCGCGCCGCCCCGGGCCAGC
AGCTCCCCGATTGGCTGAGACACTCTATATCTGGGTTGCTATCCACCCCCAAAAAAGGCAGAGAATCAACTAATGTCCTCCAG
AAATGGTTATTGGAGACTAGTATCGAATTATAGGGGATGCCTGGAGATGGTGGTGGGTTCTACCATAAGACACCAGGGCATTC
CCGTAAGCATTCAAATATGAACATCTCCTCCAGTGATAGAAATACTACCTTGGTCCAGCACACTAGTTCAGTGCAACCTCACA
TACTGAGTCTATGTGCATGTCTATGTAATTTGAACCCTATATAAGACAAGTGTGTGCTCAAAGTCGTAAATCACTGTGAACAA
ATGGCCATGGGTTGGAGTGTTTGTAACTTTGACCCTGATGCAACAAACAAACAAAAATCCAAAAGGCTTCCTTGAAAATGAAC
AAACCTGCATGTTGATGTGTTAATGTCATCAAAGAAGTACCTTTGACAAATTATGAATCAGTGTTACA

qPCR primer set:

0510B_1F-forward: TATCCACCCCCAAAAAAGGC

0510B_2R-reverse: ACCCACCACCATCTCCAGG

cDNA#: 0422E

Predicted C-type lectin domain family 4 member E:

CAGTTGGAGAGGGAGAGAGACCAGTTACAGATCAGTTATAAACGCTTGACTAAAGAAAGAGACCAGTCACAAACTCATTATAA
TACCATAACTAGAGAGAGAGACCAGTTACAAAGGAAAATTTCAGAGCAGGAGAAAAAGATATCAGAAGAACTGGGATGCTGCC
CTGGAGGTTGGAGGAGATTCGGATCTAGCTGCTATTACCTTTCAACAGAGAGTAAAACTTGGACTGAGAGCAGAGCAGACTGT
ATAAGGGGAGGGGCAGACCTGGTGATCATAAACAGCAGAGAGGAACAGGTGTTTCTAAACAAAATGGAAAAAGATGTGCGCTT
CTGGATTGGTCTGACTGACTCAGAGATGGAAGGGTTCTGGAAATGGGTGGATGGAACAACATCACCAACAACGTTCTGGAGAA
GAGGAGAGCCAAATAATGCTGATGGGGAGGAGGATTGTGTGGTATTCAACAGTTTCATTAATCTGTCTTGGGCCTGGGAAATG
ATTCAGTCATGGAATGACCAGCCTTGCTCAGTGAGTACTCAATGGGTATGTGAGAGCAGTGTCATAACAAATCCATCCACAAC
AGGAGAATAATATCTGAATTCCCTTCTGAGTTAGCAATTGTATTGTTAGTTAGCAATTGTATTATCACAGATTATTGTTGAA

qPCR primer set:

0422E_1F-forward: TAATCTGTCTTGGGCCTGGG

0422E_2R-reverse: GAGCAAGGCTGGTCATTCCA

cDNA#: 0519L

Uncharacterized predicted protein:

GAGTTTTGAGAGGTAAAGTGCGGATGAGGAGAGAAAAGTTGGTATATTAAGGAAAAAACAAGACGAAACAAATACTAAAAAAA
TTAAGGGAAGAGAAAAAAAATCAAGGAAGGTATAGAGCAGCCAGAAGCAGGGTGGTGGCAACTGGCTGCTGGTGGGCCTCCTG
GTGCCCCTCTGCATCTTCATCATTATTATTGTGGCACTGGGTATCGTCTACTGCACCCGCTGCGCCGTCATGCCGCGCAACAC
GCCGGCCACCAACTGCTACCATTGGATCTCCGGAGCGCACGACAAGCAGGGCGCGCCCAATCCCAGCAAGGGGATACAGTCAC
ATGTTTAAACAGATGAATGAGGAAAGACTTGTACATAAATAAACTGTTAAATAAATAAGAGACAGGAAGAAGGTAAGAGAGGG
GTGGTTGTTGTACTGTATCTGCCTCCTCCCGTCCCATTGCCACTGTGTTGCCGTACTGGGACTCTTTGAACACTTGAATGTGT
CTGTGGAATATCGGTTGAAAGAGAAGAACAGGGAAGCAATACTAAAAAAACGCTAATCCCTTTCATGGGGTCCTTTAGATGTG
GTAGAAAAAACGGCATAATTGTTGCTTCCACTGATCTCAAAGCACAATATATAGGCCTATGATTGCACTATAGGTACAA

qPCR primer set:

0519L_1F-forward: GCCTCCTCCCGTCCCAT

0519L_2R-reverse: GTTCAAAGAGTCCCAGTACGGC

cDNA#: 0510F

No hit:

CGTCATGCCGCGCACACGCCGGCCACCAACTGCTACCATTGGATCTCCGGAGCGCACGACAAGCAGGGCGCGCCCAATCCCAG
CAAGGGGATACAGTCACATGTTTAAACAGATGAATGAGGAAAGACTTGTACATAAATAAACTGTTAAATAAATAAGAGACAGG
AAGAAGGTAAGAGAGGGGTGGTTGTTGTACCGTATCTGCCTCCTCCCGTCCCATTGCCACTGTGTTGCCGTACTGGGACTCTT
TGAACACTTGAATGTGTCTGTGGAATATCGGTTGAAAGAGAAGAACAGGGAAGCAATACTAAAAAAACACTAATCCCTTTCAT
GGGGTCCTTTAGATGTGGTAGAAAAAACGGCATAATTGTTGCTTCCACTGATCTCAAAGCACAATATATAGGCCTATGATTGC
ACTATAGGTACAATAGAAACCGTCCATTGGGATTGTTGTTGAATACATCTGGTCATATTTACGGATGTTGTGGGAATATACTG
TCAATATATCACCAGTGCCATCTGAAACCAAAGCCAAAGAACTGTGCTGTAGCTTTTAGCATTTTTGTAGTCCATGAAATCTG
GGTGTGGGTCTTTCAAAAAAATGCTGAGGTTTTTAATGCTCAATTGAGCTCATTTCCAAGTATGTGTTGCAAATGACCATTTA
TGTCAACTTTGTTAAAGAAGGATCACATGCAGCTTCATATTTAGCTATGCAAGCTATGCAAGCATGACTGTCATGACGCTGTT

GAGGAAAAGCA

qPCR primer set:

0510F_1F-forward: TCACCAGTGCCATCTGAAACC

0510F_2R-reverse: CTAAAAGCTACAGCACAGTTCTTTGG

cDNA#: 0412C

Predicted interferon-inducible protein Gig1:

GCCACACACCGTAATAAGCTATCTCTCCATCCCATCTTTTATCATCCCTACAGTTCAAGATGGTGCGGTCTGTCAGAGAAGAA
TGTAGTCAGCTGAGCACCATACAAGACCTGAAGGACTCTGGCTTCGGCCGTCCTCCCCCCCGACACGGCCTCAAGCTCCTCTT
CTGGTTCGCCAACGAGTGCGTGGCGTTCAATCACCACGGCAACATGCTGGTAAAGTGCCACCCTGAGAGAGGCGACTTCGGCT
TCCACTACTTTGGCAACTTCGAGGAGATTCTCCCAGTTCTATCGCGAGACCGCAGGGAAAGCTACTTCGAGGTGGGCAACCTG
AACACAGAGACCTATTCCAAAGCCGAGGACCTACCGGACTACGTGAGACAGGACTACGGGCTTTCCCTGGGCTACCGCCTATG
CAACAAGGACCGCATCATCATCAGGCTGAAGCAGGGGGATGTGAAGGCCACCTATGTCACCGAGCACAAGGAGAACGGCGGCC
GGGGGGAGTTTGACTCCGAACGTACCCACCTTGTAAATCCGGATTTGATCCGCATCATCTGGGATCCTGAGCTGGAGCTAGCG
ACATTCCTGGACCAGACGGGCTACATGGGACTGTCTCCGAGAGAGCGCCTCCTCAGAGCTTTCAAGACAAACTCGGATGTCAT
CTCGTGGGAGTATGA

qPCR primer set:

0412C_1F-forward: GCATCATCATCAGGCTGAAGC

0412C_2R-reverse: TCGGTGACATAGGTGGCCTT

cDNA#: 0507O

Uncharacterized predicted protein:

ATCTGCAGTCTACTGCTGCCTCAGGACAGACACAGTCAGAGACAGTTAGAGCCACAGAGCGCGCTCAGAGACCAGCATCGCTG
CTTCTCTTTTTTTAAAGCTACACAGCCAGATCTTATCTGCACAGACGTTCATTCACAGATTCTCCTGAAGAGTTAACGAGAGA
GGCCAAACTACAGGAGCAGAGAAAAGACTTGGATATACACTATACCTTTTAATACAGCAGCCAAGAGTCCCATGTCCAAATCG
GTGTCCCAGAAGAGATTACAGCTGCCCACTATCAGCGAGGGCTACGAGGACCTGGTCAGAGACATGAACCAGACGAACCAGTC
CAACACCCTTCACTCTGCCCGGCCTACCACCCACCCAGGGCCCTGTCCACACACCCTCTCCTCAGAGGACTACCTGCTGTCCA
TCTGCCACCTGGCTCACCCCACCTCCCTTCACACCAATGGCATCATCAACCCTCATCAGCAGGTATCGCTGCACCAGAGGCCA
CGGCTGCCGCGGCTTGCTGTGCAAGATGAAAACTCTCCAAAGACCACTGCACTTTGTCCCAGGGAAAAGTCCCATGGGAAGGA
CAGGCCTGGGATGTTCTCTGACTTCATCACTGCATGCGGCAGACAGGGGAAAGATTCCAACTGCGATGAGCCTGAGTTTGGTT
GCCTTGGTGCGTCAGACCCCTTAGAGT

qPCR primer set:

0507O_1F-forward: CTGTCCATCTGCCACCTGG

0507O_2R-reverse: GATGCCATTGGTGTGAAGGG

cDNA#: 0404O

No hit:

CGCTTGACTAAAGAAAGAGACCAGTCACAAACTCATTATAATACCATAACTAGAGAGAGAGACCAGTTACAAAGGAAAATTTC

AGAGCAGTGGTATTCAACAGTTTCATTAATCTGTCTTGGGCCTGGGAAATGATTCAGTCATGGAATGACCAGCCTTGCTCAGT
GAGTACTCAATGGGTATGTGAGAGCAGTGTCATAACAAATCCATCCACAACAGGAGAATAATATCTGAATTCCCTTCTGAGTT
AGCAATTGTATTGTTAGTTAGCAATTGTATTATCACAGATTATTGTTGAAGTGTAATTTAAATCAATTATAACATTAGTTATG
ATTAGTAATGATTGTTCTTAGGATTAGTAATGATTGTTCTTAGGATTAGTAATGATTGTTCTTATGATTAGTAATGATTGTAG
TTATGATTTGGAATAATTTAATTTATATAATATAGAATTAATTATAAAGAATCATAGTATTATGAATGTGAAACTTTAACCTG
AAAGTTAATGTAGTGAATTGACATGCAGGGTCAAATCTAATCTAATCATCTAACAAGGCAAGGCAAGTGCTATGCCTCAATTT
GTGTTTATTTCTTTGTCAGATGGGATGATAATTATAGGCTACTTACTAATTCATTTTAGCTCCTAGTGGATTATATTAAATAC
ATATTTTGAAAG

qPCR primer set:
0404O_1F-forward: GTGAATTGACATGCAGGGTCA
0404O_2R-reverse: TTGAGGCATAGCACTTGCCTT

cDNA: Predicted aquaporin4

GGCATGGATCATTTTCATCGGACAGACCCACTACTACTTTCTCCTCCCGTCTCGCACTGTGTCATTACCAGCCAACTGCTGCC
TGTCTGAGCTGCCTGTCGGCGTGTAACCAGCATCCCATGATGGTGGCATTCAAAGGAATCTGGACCAAGAACTTCTGGAGGGC
TGTCTCAGCTGAGTACCTAGCAACCACGATCTTCGTCCTCCTCAGCCTGGGCTCCACCATCAATTGGGCGGCCGAGTCAGACA
ACCCTCCCCCTGCAGACCTGGTCCTCATCTCATTTTGCTTCGGGCTGTCCATTGCCACAATGGTGCAGTGCTTTGGTCACATC
AGCGGTGGCCACATCAACCCGGCAGTCACTGCAGCCATGGTGGTGACCCGGAAGTTGAGCCTGGCCAAGGGTGTGTTCTACCT
AGCTGCCCAGTGCCTGGGGGCGATCACTGGGGCAGGGCTCCTCTACCTGGTGACGCCAGTGTCTGTCAGAGGGGGCCTGGGCT
GCGGCCTGTTGGTGGAGCTCCTGATCACCTTCGAGCTGGTCTTCACGGTGTTCGCCACCTGTGACCCCAAACGCTCTGTTAAC
GGCTCGGCTGGCCTCGCCATCGGATTCGCTGTAGCCATCGGTCATCTGTTCGCAATTCCATACACAGGAGCCAGTATGAACCC
CGCTCGCTCCTTTGGACCTGCAGTCGTCACCATGAACTTTGAGAACCACTGGGTGTACTGGGTTGGCCCAATCCTGGGT

qPCR primer set:
aquapolin4-1F-forward: TGGATCATTTTCATCGGACAGA
aquapolin4-2R-reverse: GCGAGACGGGAGGAGAAAGTA

cDNA: Predicted lectin

GATCAGTTATAAACGCTTGACTAAAGAAGAGACCAGTCACAAACTCATTATAATACCAtAACTAGAGAGAGAGACCAGTTACA
AAGGAAAATTTCAGAGCAGGAGAAAAAGATATCAGAAGAACTGGGATGCTGCCCTGGAGGTTGGAGGAGATTCGGATCTAGCT
GCTATTACCTTTCAACAGAGAGTAAAACTTGGACTGAGAGCAGAGCAGACTGTATAAGGGGAGGGGCAGACCTGGTGATCATA
AACAGCAGAGAGGAACAGGTGTTTCTAAACAAAATGGAAAAAGATGTGCACTTCTGGATTGGTCTGACTGACTCAGAGATGGA
AGGGTTCTGGAAATGGGTGGATGGAGCGACATCACCAACAACGTTCTGGAGAAGAGGAGAGCCAAATAATGCTGATGGGGAGG
AGGATTGTGTGGTATTCAACAGTTTCATTAATCTGTCTTGGGCCTGGGAAATGATTCAGTCATGGAATGACCAGCCTTGCTCA
GTGAGTACTCAATGGGTATGTGAGAGCAGTGTCATAACAAATCCATCCACAACAGGAGAATAATATCTGAATTCCCTTCTGAG
TTAGCAATTGTATTGTTAGTTAGCAATTGTATTATCACAGATTATTGTTGAAGTGTAATTTAAATCAACTATAACATTAGTTA
TGATTAGTAATGATTGTTCTTAGGATTAGTAATGATTGTTCTTAGGATTAGTAATGATTGTTCTTATGATTAGTAATGATTGT
AGTTATGA

qPCR primer set:

lectin-1F-forward: TTCTGGAAATGGGTGGATGG

lectin-2R-reverse: GAATACCACACAATCCTCCTCCC

cDNA#: 0503I, Predicted mevalonate (diphospho) decarboxylase

(A)

The number of reads:

ID	cont	fors
fors_65039	0	23
fors_124871	1	18
mixed_29426	0	6
fors_53103	1	25
mixed_34741	2	6
fors_56281	3	55

(B)

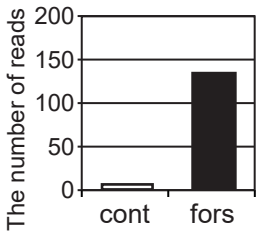

(C)

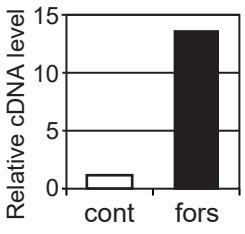

(D)

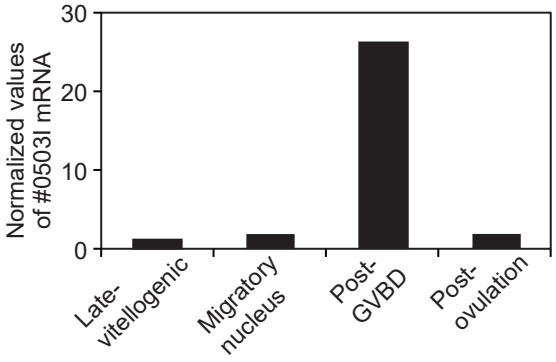

cDNA#: 0414B, Unknown

(A)

The number of reads:

ID	cont	fors
fors_42965	7	221
mixed_22700	7	241

(B)

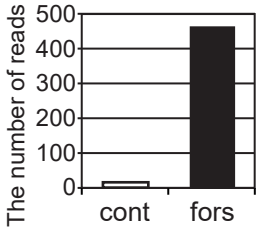

(C)

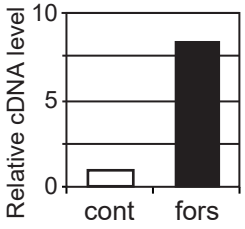

(D)

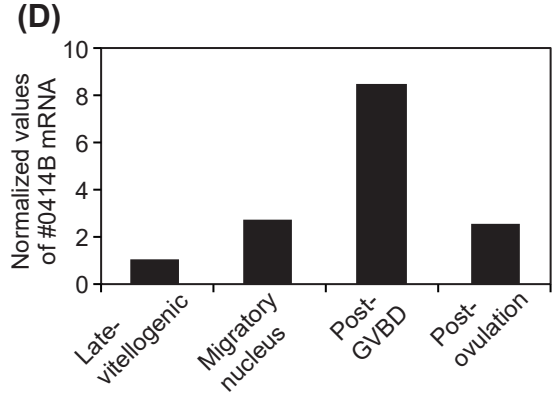

cDNA#: 0509L, Predicted cAMP-dependent protein kinase catalytic subunit beta

(A)

The number of reads:

ID	cont	fors
mixed_23411	67	268

(B)

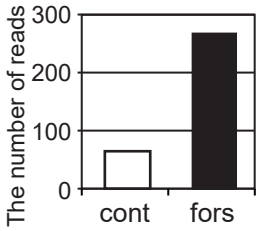

(C)

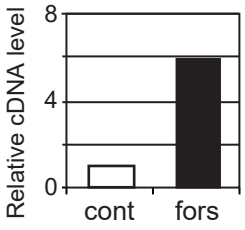

(D)

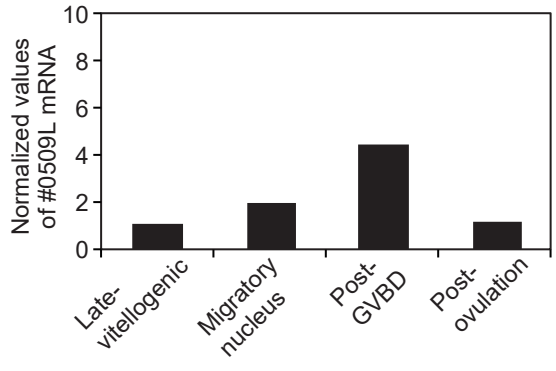

cDNA#: 0408O, Predicted CREB cAMP responsive element modulator

(A)

The number of reads:

ID	cont	fors
fors_29520	3	280
fors_19488	1	107
fors_74257	0	25

(B)

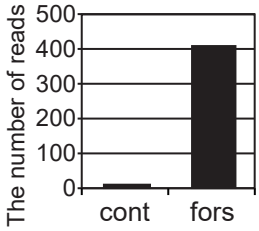

(C)

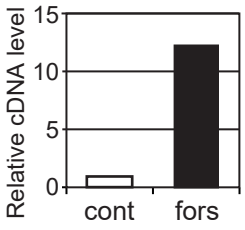

(D)

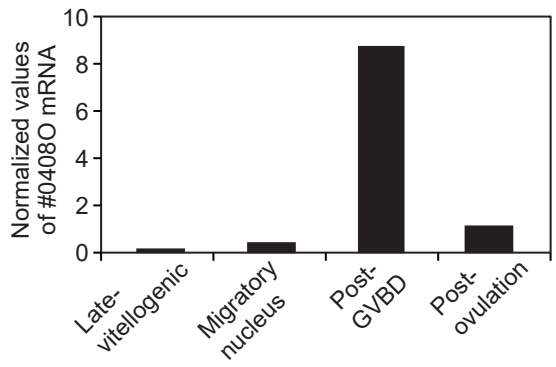

Supplemental Fig. 4(1)

cDNA#: 0510B, Predicted phosphatase, orphan 1

(A)

The number of reads:

ID	cont	fors
fors_144864	0	9
fors_199070	0	12
fors_44676	0	17

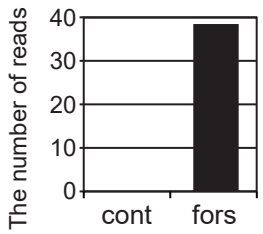

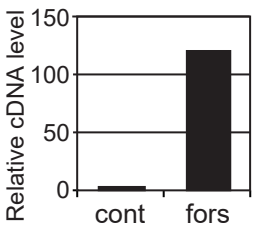

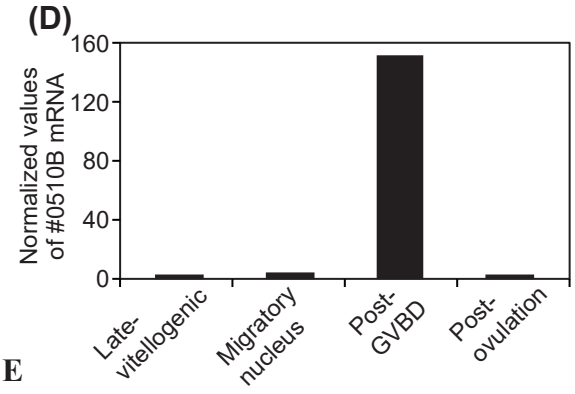

cDNA#: 0422E, Predicted C-type lectin domain family 4 member E

(A)

The number of reads:

ID	cont	fors
fors_185398	0	11

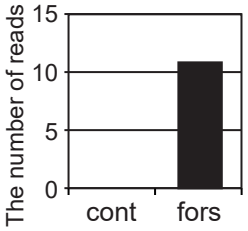

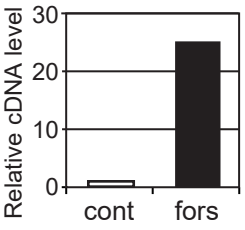

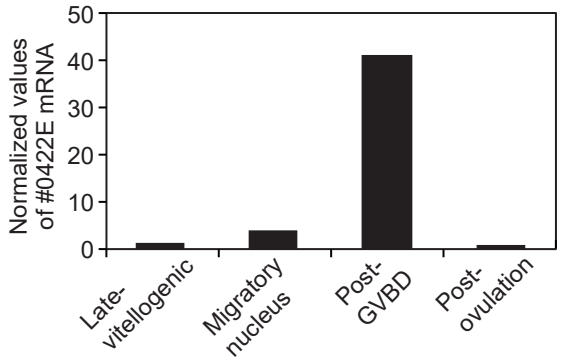

cDNA#: 0519L, Uncharacterized predicted protein

(A)

The number of reads:

ID	cont	fors
fors_101202	3	24

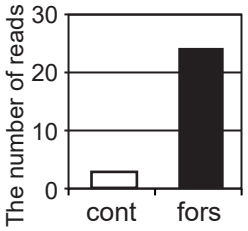

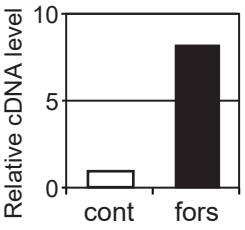

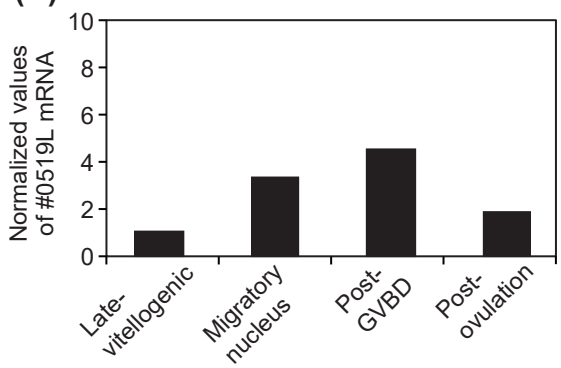

cDNA#: 0510F, No hit

(A)

The number of reads:

ID	cont	fors
mixed_6494	2582	12834
fors_101202	3	24
mixed_4260	125	830

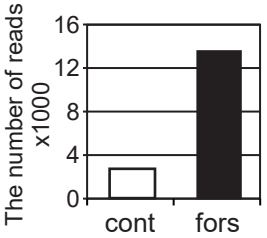

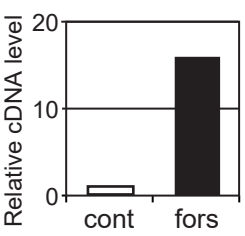

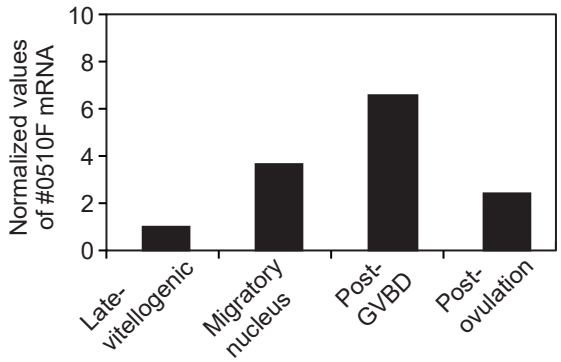

cDNA#: 0412C, Predicted interferon-inducible protein Gig1

(A)

No matching contig:

ID	cont	fors

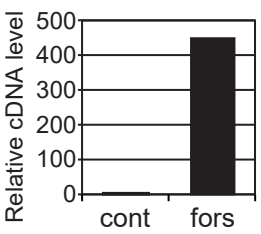

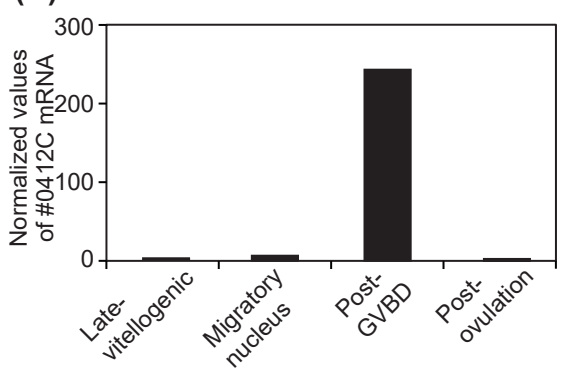

Supplemental Fig. 4(2)

cDNA#: 0507O, Uncharacterized predicted protein

(A)

The number of reads:

ID	cont	fors
fors_144550	4	11

(B)

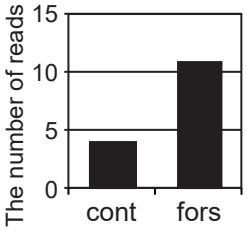

(C)

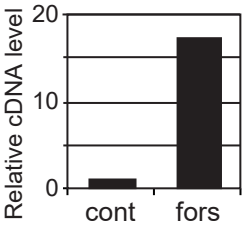

(D)

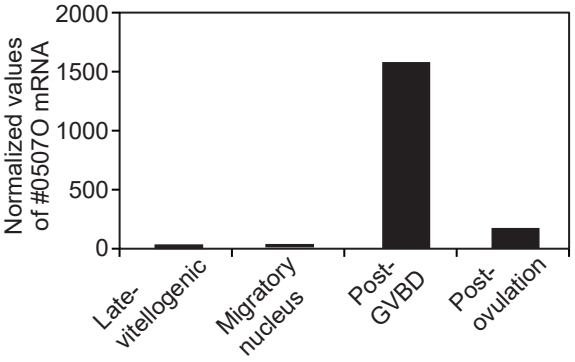

cDNA#: 0404O, No hit

(A)

The number of reads:

ID	cont	fors
fors_46026	0	23

(B)

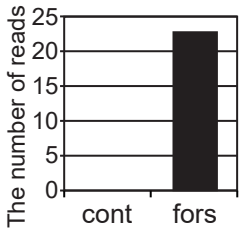

(C)

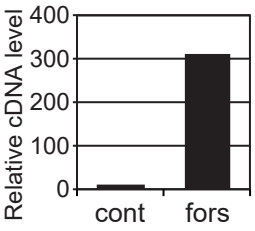

(D)

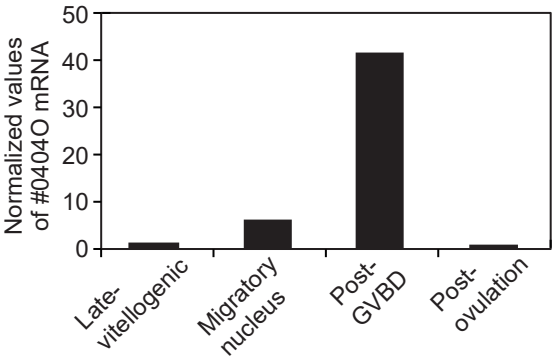

cDNA: Predicted aquaporin4

(A)

No matching contig:

ID	cont	fors

(C)

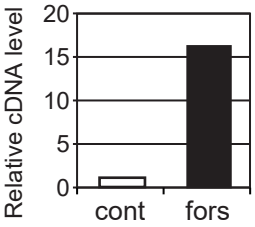

(D)

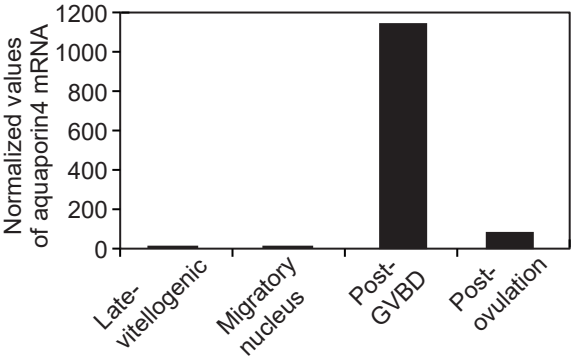

cDNA: Predicted lectin

(A)

The number of reads:

ID	cont	fors
fors_33829	1	437

(B)

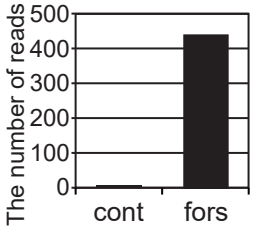

(C)

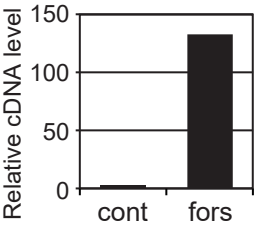

(D)

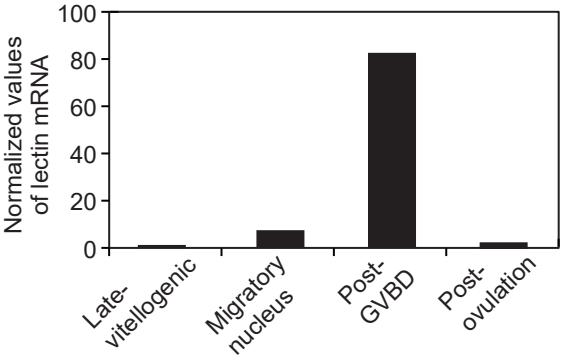

Supplemental Fig. 4(3)

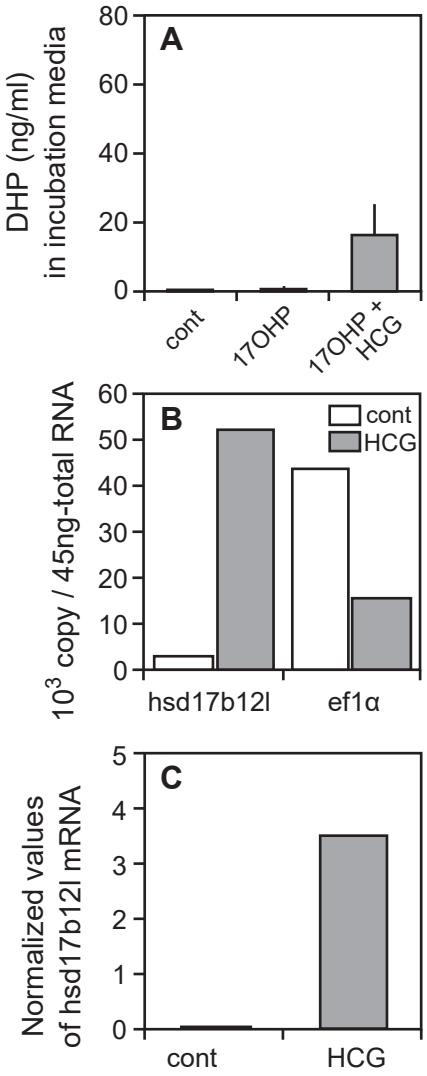

Supplemental Fig. 5